AD-A058 829 WASHINGTON UNIV SEATTLE LAB FOR CHEMOMETRICS F/G 9/3
MINICOMPUTER-CONTROLLED, BACKGROUND-SUBTRACTED ANODIC STRIPPING--ETC(U)
AUG 78 S D BROWN, B R KOWALSKI N00014-75-C-0536

UNCLASSIFIED NL

1 OF 1
AD A058 829

END
DATE FILMED
-11-78
DDC

UNCLASSIFIED

SECURITY CLASSIFICATION OF THIS PAGE (When Data Entered)

REPORT DOCUMENTATION PAGE

READ INSTRUCTIONS BEFORE COMPLETING FORM

1. REPORT NUMBER	2. GOVT ACCESSION NO.	3. RECIPIENT'S CATALOG NUMBER
12	--	--

4. TITLE (and Subtitle)
Minicomputer-controlled, background-subtracted Anodic stripping voltammetry: evaluation of parameters and performance

5. TYPE OF REPORT & PERIOD COVERED
Technical - Interim
2-78 - 8-78

6. PERFORMING ORG. REPORT NUMBER
--

7. AUTHOR(s)
Steven D. Brown
Bruce R. Kowalski

8. CONTRACT OR GRANT NUMBER(s)
N00014-75-C-0536

9. PERFORMING ORGANIZATION NAME AND ADDRESS
Laboratory for Chemometrics, Department of Chemistry, University of Washington, Seattle, Wash, 98195

10. PROGRAM ELEMENT, PROJECT, TASK AREA & WORK UNIT NUMBERS
NR 051-565

11. CONTROLLING OFFICE NAME AND ADDRESS
Materials Sciences Division
Office of Naval Research
Arlington, Virginia 22217

12. REPORT DATE
August 1978

13. NUMBER OF PAGES
37

14. MONITORING AGENCY NAME & ADDRESS (if different from Controlling Office)
--

15. SECURITY CLASS. (of this report)
UNCLASSIFIED

15a. DECLASSIFICATION/DOWNGRADING SCHEDULE

16. DISTRIBUTION STATEMENT (of this Report)
Approved for public release; distribution unlimited

17. DISTRIBUTION STATEMENT (of the abstract entered in Block 20, if different from Report)
--

18. SUPPLEMENTARY NOTES
Prepared for publication in Analytical Chemistry

19. KEY WORDS (Continue on reverse side if necessary and identify by block number)
anodic stripping voltammetry
linear scan
differential voltammetry
digital subtraction

20. ABSTRACT (Continue on reverse side if necessary and identify by block number)

A new minicomputer controlled anodic stripping voltammetry technique is described. The technique uses differential voltammetry on one electrode and uses a rapid data averaging algorithm to avoid the need for scan averaging, allowing excellent sensitivities and short analysis times, with adequate reproducibilities. Both linear scan and staircase waveforms are discussed and the approximate Roe-Toni theory for linear scan voltammetry is shown to apply. The viability of the technique in solutions showing a large background is also discussed.

DD FORM 1 JAN 73 1473 EDITION OF 1 NOV 65 IS OBSOLETE
S/N 0102-014-6601

SECURITY CLASSIFICATION OF THIS PAGE (When Data Entered)

OFFICE OF NAVAL RESEARCH

(15) Contract N00014-75-C-0536

Task No. NR 051-565

(6) MINICOMPUTER-CONTROLLED, BACKGROUND-SUBTRACTED ANODIC STRIPPING VOLTAMMETRY: EVALUATION OF PARAMETERS AND PERFORMANCE,

Prepared for Publication

in

Analytical Chemistry

by

(10) Steven D. Brown
and
Bruce R. Kowalski
Laboratory for Chemometrics
Department of Chemistry, BG-10
University of Washington
Seattle, Washington 98195

(11) Aug[redacted]978 (12) 67p.

ABSTRACT

A new minicomputer controlled anodic stripping voltammetry technique is described. The technique uses differential voltammetry on one electrode, and uses a rapid data averaging algorithm to avoid the need for scan averaging, allowing excellent sensitivities and short analysis times, with adequate reproducibilities. Both linear scan and staircase waveforms are discussed in conjunction with the technique, and the approximate Roe-Toni theory for linear scan voltammetry is shown to apply. The system response is investigated for film thickness, scan rate, deposition time, electrode rotation rate, and metal concentration. Results were used to optimize the experiment sensitivity. The metals Cd, Pb and Cn could be analyzed in solutions as dilute as 1-10 pg/ml in fifteen minutes. The viability of the technique in solutions showing a large background is also discussed, and a comparison is made with scan-averaged techniques.

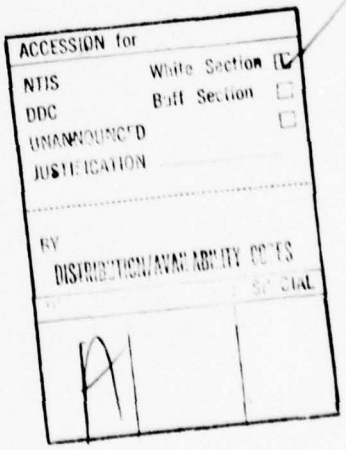

A variety of approaches have been proposed with the aim of reducing the time of analysis using the anodic stripping voltammetry (ASV) technique. These include the use of flow systems (1-3), thin film electrodes (4), pulse and differential pulse techniques (5-11), and rotating disk electrodes (12-14), ring-disk electrodes (15-16), and recently, computer controlled instrumentation (17-22). In a few cases, analysis times were actually decreased, but the majority of the techniques mentioned above still utilize either long electrolysis times or long stripping times, and the actual time savings for realistic metal concentrations (i.e., in the parts-per-billion range and below) is small.

Both the sensitivity of the ASV technique and the overall analysis time depend upon how the capacitive current contribution to the total current is removed or compensated. One approach to eliminating the capacitive contribution to the total current utilizes the concept of differential voltammetry. Here, an attempt is made to actually measure the purely capacitive current, and to subtract it from the simultaneously measured total current, yielding only the faradaic current. This can be done using two electrodes, one of which is placed in a solution having no depolarizer, so no material deposits on the electrode, and essentially no faradaic current flows during a potential scan. The other electrode, placed in the analyte solution, passes both faradaic and capacitive currents during the potential scan, allowing either electronic or digital subtraction of the current generated by the first electrode from the second (23-25).

The above technique and the more common pulse technique are significantly better than simple linear scan ASV, but both have serious disadvantages. Pulsed techniques require much slower scan rates than are feasible with linear scans, in order to allow the differential current decay, upon which

pulse techniques are based. Thus, although they may not require the long deposition times needed for linear scans, they frequently require long stripping times. Additionally, by sampling after a delay, some of the faradaic current is lost, resulting in a somewhat lowered sensitivity. This has been observed for the staircase waveform in particular (21). Differential voltammetry techniques do not "throw away" faradaic current, and are therefore quite sensitive. Both the capacitive and faradaic currents are particularly sensitive to the exact electrode surface area, however. Since no two electrode surfaces match exactly, the capacitive current is generally not well compensated; peaks come out poorly defined and run-to-run reproducibility is poor. Differential techniques thus allow rapid scans in theory, but results are poor in practice (26). A related technique, using a split electrode with separately controllable potentials (25), gives similar results.

Recently, however, work has appeared on another method which is a variant of differential voltammetry, but uses only one electrode. Here, one normal ASV run with deposition step, rest period and stripping step is performed. Immediately after this ASV run, however, the potential of the working electrode is switched to some potential where no depolarizer plates into the mercury, but where the mercury itself is not undergoing dissolution. Potentials slightly cathodic of 0 mv versus the saturated calomel electrode (S.C.E.) are suitable. Stirring is begun, and after a set time called the cleaning period, the potential of the working electrode is switched to the rest potential. After a short time at the rest potential, the electrode is again scanned anodically, exactly as in the stripping step of the previous ASV run. Since this scan produces essentially no faradaic current, primarily capacitive currents are observed. Thus, digital subtraction of this scan,

called the background scan, from the first scan, the analyte scan, essentially removes the capacitive current contribution from the total current, and leaves only faradaic current. The advantage over two-electrode differential voltammetry is that the electrode surfaces match exactly, and the process of compensation is both reproducible and essentially complete. This technique was first used for linear scan ASV by Kryger and Jagner (17-19) who combined it with a normalized averaging of multiple stripping steps; that is, 40 rapid scans were performed first for the analyte scan, added, normalized, and stored. The background was recorded by scanning another 40 times, adding the scans and normalizing the scans. Subsequent subtraction of the normalized sum of background scans from the analyte scans yielded the background corrected multiple scan ASV (MSASV) scan. The technique was fairly rapid, sensitive, very reproducible, and especially useful for elements like Bi, which has a dissolution potential of -100 mv vs the S.C.E., putting it on the shoulder of the enormous mercury stripping peak caused by dissolution of the TFME.

Other waveforms can also be used. Both the square wave and staircase waveforms have been used in conjunction with background subtraction (22). Here, only one analyte scan and one background scan were used. No detailed work was given with these waveforms in conjunction with background subtraction, however.

Because the technique of background subtraction using one electrode relies upon digital storage of the analyte scan and the background scan, with a subsequent point-by-point subtraction of the background, computerized data acquisition is clearly desirable. Control of the experiment through the potentiostat is also desirable, as operator intervention can be reduced to a minimum, increasing reproducibility and greatly simplifying an analysis.

Rather little work has appeared, however, on computer-controlled ASV experimentation, despite the fact that a commercial microprocessor-controlled instrument is now available (the PAR 374). Bond, et al. (20,27) have evaluated the performance of the PAR 374, which has the capability of performing blank subtraction. Using the HMDE, they were able to obtain peak height reproducibilities of ±1% for Pb at the 10^{-7} M (20 ng/ml) level in 0.1 M KNO_3. This was considerably better than conventional instrumentation, which showed reproducibilities of ±3% for identical conditions. Background subtraction was not used for these determinations.

A minicomputer has also been used for the optimization of ASV experimental parameters (28). The computer controlled a home-built potentiostat and attempted to control experimental conditions to meet preselected performance criteria.

Less sophisticated control, via a minicomputer, of commercial potentiostats, such as the PAR 173 and PAR 174, has been used in reports on staircase ASV (21,22). The use of FORTRAN program-based, computer-generated waveforms is quite straightforward in this case. Reproducibilities for Cd at the 10^{-7} M (10 ng/ml) level in 0.01 M acetate buffer were ±1% on the same thin film, and ±5% on repeated thin films, again superior to conventional techniques. As discussed above, background subtraction has also been briefly examined for this system.

Control via a large computer through a timesharing system has also been reported by Kryger and Jagner (17-19) in their MSASV studies. There, an RC 4000 computer was used to control the potentiostat and collect data through a low-speed channel. The computer was also interfaced to the stirrer and to a digital burette, so that the entire experiment was under computer control. A flexible program written in SLANG (an assembly language), callable from the ALGOL-based main program, was used to generate a variety of wave-

forms, to perform the normalized scans and to subtract the background. Analyses of Cd at the 10^{-8} (1 ng/ml) level showed an average deviation of less than ±2% for duplicate measurements, far superior to conventional techniques.

This paper describes a new computer-controlled voltammeter that uses a single, rapid scan to measure currents, and a second, rapid background scan to compensate for the large capacitive contribution generated by a fast scan. Deposition times are minimized by using a large rotating disk electrode, which along with the digital removal of the background currents, greatly assists in improving the reproducibility of the technique and in substantially reducing the times required for analysis by the techniques.

THEORY

For thin film mercury electrodes, the exact theory developed by DeVries and vanDalen (29, 30, 31) and a more approximate theory proposed by Roe and Tony (32) may be applied. Both are based on a linear scan. The theory for staircase scan (33) and differential pulse (33) ASV has been derived by Christie and Osteryoung. These will be discussed here only briefly.

The Roe and Toni relationships for peak current and peak potential are given by equations 1 and 2:

$$i_p = nFA\ell C_R^o \nu \cdot \frac{nF}{RTe} \tag{1}$$

$$E_p = E^{o'} + 2.3 \frac{RT}{nF} \log \frac{nF\delta\ell\nu}{RTD_{ox}} \tag{2}$$

The nomenclature here is identical to that of Roe and Toni (32). These equations apply to a linear scan ASV experiment with a fixed diffusion layer

thickness δ, generated by rotating the electrode during the scan.

For staircase scan ASV, equivalent relationships are given by equations 3 and 4:

$$i_p = g_p' \frac{n\Delta E}{\tau} q_m \tag{3}$$

$$E_p = E^{o'} + \frac{2.3}{nF} \log \frac{1^2}{D\tau} + K \tag{4}$$

where g_p' is a "normalized stripping function," ΔE is the step height, τ is the delay time, and K is a constant.

Both the DeVries-vanDalen and the Roe-Toni theories have been experimentally verified (31, 32) for thin films and slow scans. In the limit of fast linear scans, they can be reduced to the Randles-Ševčik theory for rapid linear scan voltammetry (35,36). The theory for staircase voltammetry has also been tested in relatively concentrated (20 ng/ml) solution (21).

Examination of the Roe and Toni equations (equations 1 and 2) suggests that, by using a fairly large electrode surface area and a fast scan rate, large faradaic currents will be obtained. Results obtained by DeVries (30) indicate that a thin film is needed when a fast scan rate is used, in order to keep adequate resolution, which otherwise degrades substantially. Thus, a very fast scan rate, on the order of 1000-3000 mv/sec, used in conjunction with an electrode of high surface area but low volume, should maximize the peak current, thus allowing shorter deposition times. A decrease in the effective diffusion layer, obtained by rotation of the electrode during the stripping step, theoretically should increase (by $\sim$24%) the peak currents (31), but this has been shown (37) not to be true, primarily due to the increased noise generated by the stirring process.

During the deposition step, however, rotation of the electrode will substantially increase the amount of material plated onto a disk electrode according to the well-established Levich equation (38) for the instantaneous current of a mass transport-controlled reaction:

$$i_p = 0.62nFA\ C^o_{ox} D^{2/3}_{ox}\ \rho^{-1/6}\omega^{1/2} \qquad (5)$$

where ρ is the kinematic viscosity of the solution (in cm^2/sec) and $\omega = 2\pi f/60$ where f is the rotation speed in r.p.m.

High scan rates generate large capacitive currents in addition to large faradaic currents, and these currents must be removed. Background subtraction is an obvious choice to accomplish this. A modification of the technique used by Kryger and Jagner (17-19) was chosen as the means of accomplishing background subtraction. Computer control was implemented to take advantage of the better precision obtainable with automated instrumentation, as well as to simplify the analysis.

The system described above should maximize the sensitivity and minimize the analysis time of the ASV technique, because the limit of detection of the technique is large determined by the uncertainty in the determination of the current, due to current contributions of processes other than the stripping of the desired species. These "background" processes include, in addition to the capacitive current already discussed, the electrochemical reactions of the electrode itself, such as oxidation of the mercury film, or evolution of hydrogen. By performing the subtraction of a blank scan, made by the process described above, one is able to remove the effects caused by these background processes virtually completely, decreasing the uncertainty in evaluating peak currents, and substantially lowering the detection limit. This should have the effect of allowing much shorter analysis times than the conventional technique.

EXPERIMENTAL

Cell and Electrodes

The working electrode used was a commercial RDE, model DD-20, from the Pine Instrument Company of Grove City, Pennsylvania. The body of the electrode was Teflon, and the disk was glassy carbon. Polishing, which is critical to electrode performance (12), was done as follows: After initial polishing with strips of #600 carborundum paper, careful polishing for 2 to 3 hours with a suspension of 0.5μm alumina (Buehler AB Alpha Polishing Alumina) on sebyl cloth was performed to generate a smooth surface. Subsequent gentle polishing with a suspension of 0.05μm alumina (Buehler AB Gamma Polishing Alumina) on wet filter paper was used to obtain a mirror-like finish. At the start of a series of runs, the electrode was briefly repolished with the 0.05μm alumina suspension to insure a relatively constant electrode surface area. The nominal surface area of the disk was 0.45 cm^2.

The electrode was held in a Pine Instrument Company rotator, model ASR. The rotator had its lower electrode contact removed to avoid contamination of the solution with silver-loaded graphite particles (15). The electrode was rotated at speeds ranging from 1,000 - 10,000 rpm via voltages applied to the external input by one of the digital to analog converters provided on the computer interface, and thus was under computer control. A check was made of the accuracy and precision of the speed of the rotation by monitoring the external output voltage of the rotation servo-mechanism circuit. Accuracy was within 1% and reproducibility was better than 0.2% when computer control was used.

The reference electrode was a Princeton Applied Research saturated calomel electrode. Electrical contact was made with the test solution by means of a bridge filled with either saturated KCl, KNO_3, or NH_4NO_3 solution.

The bridge tube was provided with a Vycor frit to contact the test solution; this frit was sealed into a length of heat-shrinkable Teflon tubing, so that only the frit and Teflon contacted the test solution. The upper portion of the bridge tube was glass.

The counter electrode was a length of heavy gauge Pt wire bent into a small spiral and sealed into a glass ground joint.

The purge tube was a Princeton Applied Research Corporation model 9330 unit, bent to fit under the rotator. The purge tube contacted the test solution via a length of rigid 2mm Teflon tubing.

The cell was a modified 200 ml clear fused silica beaker from Quartz Scientific, of Sunnyvale, California. The top of the beaker was removed to make a container 65mm in diameter by 70mm in height. The capacity of the cell was 125 ml, but normal analysis volumes were 65 - 80 ml. The reference and counter electrodes, as well as the purge tube, were held by a Teflon cover for the cell, which was also provided with a glass-stoppered port to allow easy access to the test solution for addition of reagents. The rotating disk working electrode fit through a central opening in the cover; an annular space was provided to allow gas to exit the otherwise airtight cell. The cell was not thermostated, but temperature fluctuations in the room were minimal.

Instrumentation

All measurements were made with a potentiostat designed to be controllable with the computer and computer interface combination.

Computer Interface. A general purpose interface was built to allow a variety of instrumentation to be serviced by the laboratory computer. The interface has been described previously (39) but a brief description will be repeated here for clarity. The interface, diagrammed in Figure 1,

consists of six devices on the UNIBUS of our PDP-11/05 minicomputer (40). All devices have 18-bit addresses to allow compatibility with the larger PDP-11 computers.

Data acquisition capability is provided by a Datel MDAS-16 system which consists of a 16-channel analog multiplexer, monolithic sample and hold amplifier and a 6μsec, 12-bit successive approximation analog-to-digital converter (ADC), of which only one channel was required here. Input voltages may range from +10v to -10v, giving a resolution of 4.88 mv. The maximum throughout was 57.1 KHz, with an error of ±0.015% of full scale response. The ADC could be started manually or by underflow of clock #2, allowing very precisely-timed sampling. An extra data latch was provided for the ADC to allow ADC restart without loss of data that would otherwise be caused by the new conversion. The ADC unit was provided with interrupt capability (40) to allow the computer to perform other tasks while sampling, and to allow more precise time control.

The interface is provided with four digital output functions called logic levels. These outputs, which provide +3.5v when a logic "1" is loaded into the bit corresponding to that output, and 0.0v otherwise, may be used to set the gain of an external experiment. Logic pulses are also provided, but they were not used in this work, and will not be discussed here.

A six-digit decimal display is also provided. Coding for the display is in binary-coded decimal (BCD) and conversion of binary bits to BCD must be done by the software.

The interface is provided with relays and switched 115 VAC outlets. The relays, of SPDT type, have a settling time of approximately 1 msec, and are useful for a variety of control functions. Here, one relay was

used to switch a field effect transistor which was provided to start and stop the linear scan analog ramp, as will be discussed below.

Analog output from the interface is accomplished by four digital-to-analog converters (DACs). The 12-bit DACs were equipped with switchable ranges, including ±10v, ±5v, and ±2.5v bipolar scales, as well as +10v and +5v unipolar scales. Settling time for the DACs were observed to be less than 40μsec, and linearity was better than 0.25%. Three of the DACs were used in this work, two of which supplied the potentiostat with control voltages, and one of which supplied the ASR rotator with a voltage proportional to the speed of electrode rotation.

The interface is equipped with three variable time base, programmable clocks. Basic periods available range from the oscillator time of 1μsec to as long as 100 sec, scaled by decades. A 12-bit countdown buffer is also provided to allow any period between the basic ones provided. The clocks automatically decrement this buffer, and reload it upon underflow (except when in the elapsed time mode). Clock #2 is capable of starting the ADC upon underflow, and all clocks have interrupt capability to allow accurate timing of a process while other tasks are being handled. In this work, clock #0 was used as the basic timer, and clock #2 was used to control the sampling rate of the ADC. Clock #1 was used to generate the delay time in the staircase stripping experiments.

Other features of the interface, including the Schmitt triggers, sense switches, contact closures, and a 16-bit parallel input-output port were not used, and will not be discussed here.

Computing System. The interface discussed above was connected to a Digital Equipment Corporation (DEC) PDP-11/05 GT-40 minicomputer equipped with 24K core memory and hardware arithmetic capability. This computer,

usually used as a "smart" terminal, was modified to fit a standard 19-inch relay rack, also purchased from Digital Equipment, of Maynard, Massachusetts. The control boards for the interface and for other peripherals were held in a modified DEC BA11-ES extension box built into the relay rack. Mass storage was provided by a DEC RX-01 dual-drive, single density floppy disk system, and serial input-output was handled by two DEC DL-11 ports provided on the PDP-11/05. The baud rate for one port was made selectible, to allow use of a 9600 baud Tektronix model 4012 graphics terminal from Tektronix, Beaverton, Oregon, or to access the CDC 6400 computer, located in the University Computing Center, via a 1200 baud modem. Hard copy of experimental results could be obtained either from a Gould 5000 printer-plotter connected to our PDP-11, or from a large Calcomp plotter at the Academic Computer Center, University of Washington.

The operating system for the PDP-11/05 was Digital Equipment Corporation's RT-11 single job monitor (56). Versions 2C and 3 were used. Plotting software was provided by Gould for use with the 5000 plotter, but was modified to allow use with the Tektronix terminal as well.

Computer Controlled Potentiostat. The potentiostat used to perform the voltammetric experimentation was designed and built by the author to be directly compatible with the computer/interface system outlined above. Figure 2 details the schematic diagram of the potentiostat, which is of conventional three-electrode design (42-47). DAC 1 is used to provide the electrolysis potential, which also acts as a baseline for the scan. The output scale used is ±2.5v, allowing a resolution of 1.22 mv. DAC Ø is used to provide a voltage proportional to the desired scan rate, when linear scan voltammetry is being performed. The output scale here is +5v, again allowing a resolution of 1.22 mv. For the staircase scan technique,

DAC 1 actually generates the staircase directly, as one might expect. Waveforms were monitored with a Tektronix T935 oscilloscope. The relay input is used to switch the field effect transistor, which connects (or shorts) the capacitor on the integrator, triggering (or resetting) the linear scan. The two logic level inputs select the current-measuring feedback resistor by switching a CMOS demultiplexer; they are amplified by the two transistors because the TTL interface outputs are not directly compatible with the CMOS voltages. The CMOS demultiplexer was an RCA CD4051 chip (48). Current ranges available are given in Table 1. The output of the reference electrode amplifier was monitored with a Data Precision Model 175 digital voltohmmeter to obtain the potential applied to the working electrode. All the operational amplifiers are RCA 3041T types, chosen for their fast settling time, high gain, and high input resistance (48). The potentiostat was housed in a 13 x 9 x 8 inch Vector Multi-Mod steel box for shielding, and the rotator, cell and potentiostat were placed in a Manostat Glove Box (VWR #32981-003) for protection from dust. The entire unit was mounted on a large lab cart (Fisher #11-932) for portability, with all electrical power supplied via a multiple outlet box made by SGL Waber electric of Westville, N. J., to provide a common ground.

With this potentiostat, a variety of waveforms can be applied to the cell, including linear scan and a number of square wave-based functions. In this study, however, only linear scan and staircase waveforms were used. Linear scan rates of up to 5000 mv/sec were possible, but all work used rates of 100 - 3000 mv/sec. Scan rates are essentially continuously variable, differing by at least 1.22 mv/sec, the resolution of the DAC scale used to supply the rate voltage. Staircase step heights based on multiples of 1.22 mv/step were possible. Usually, step heights of 4.88 mv were used to obtain

reasonable sensitivity as well as good peak resolution (48), since large step heights degrade peak resolution, while small step heights are significantly less sensitive.

The band width of the potentiostat was measured by the method of Booman and Holbrook (42), and showed a -3db cutoff at 14 KHz.

Reagents

The HCl and HNO_3, as well as the KCl were Ultrex grade, from the J. T. Baker Co. The KNO_3, CH_3COONa and CH_3COOH were Baker Analyzed Reagents. Mallinckrodt $HClO_4$ and $NaHCO_3$ (AR grade) were also used. Airco prepurified N_2 further purified by passage through a gas washing bottle containing V(II) ions, and a second gas washing bottle containing supporting electrolyte, was used to remove oxygen from the test solution.

The Hg(II) plating solution was prepared by dissolving Baker Instrumental Grade Hg in a minimum amount of Ultrex HNO_3, and diluting to give a 0.01M solution of $Hg(NO_3)_2$.

An Au(III) plating solution was prepared by dissolving Alpha-Ventron m6N purity Au powder in a minimum of a mixture of 3 parts Ultrex HCl and 1 part Ultrex HNO_3, heating gently to expel nitrogen oxides and nitrosyl chloride, then diluting to give a 2×10^{-4} M solution of $HAuCl_4$.

Standard solutions of As were prepared by dissolving Alpha-Ventron ultrapure As_2O_3 in a minimum of a 10% $NaHCO_3$ solution, then adding HCl and diluting to make a 1000 ppm As(III) solution in 1N HCl.

Standard solutions of Cd and Zn were prepared by dissolving Alpha-Ventron ultrapure $CdCO_3$ and ZnO in a minimum of Ultrex HNO_3, heating, and diluting to make 1000 ppm solutions of $Cd(NO_3)_2$.

Standard solutions of Cu were obtained by dissolving m2N5 purity Cu metal (Alpha-Ventron) in a minimum of Ultrex HNO_3, heating, and diluting to make a 1000 ppm solution of $Cu(NO_3)_2$.

Standard solutions of Pb were prepared by dissolving ultrapure Pb $(CH_3COO)_2 \cdot 3H_2O$ in a minimum of Ultrex HNO_3 , evaporating to dryness to remove acetic acid, and diluting to make a 1000 ppm solution of $Pb(NO_3)_2$.

All solutions were prepared with water purified by passage through a high-efficiency, mixed bed ion-exchanger (Corning 3508-B) and subsequently distilling in a Corning AG-2 still. Distilled water and all solutions were stored in thoroughly pre-leached linear polyethylene bottles to avoid severe contamination (47-50). Analysis of water prepared in this way, by the ASV technique reported here, showed metal concentrations well below ppb levels, with the primary contaminant being Zn, probably due to atmospheric fallout. The water was used within 72 hours.

For studies on the sensitivity of the technique, specially purified water was prepared by repetitively distilling the distilled water, collecting it in a thoroughly pre-leached (with Ultrex HCl and HNO_3) Teflon FEP 1 liter bottle. This water was used at once.

For all studies, the solutions of buffers used as supporting electrolytes were carefully purified by prolonged electrolysis over a mercury pool in a Princeton Applied Research electrolytic purification unit, using a PAR 174A as the means of controlling the potential. Electrolyses usually spanned 2 to 3 weeks at a potential of at least -1.6V versus the SCE. These solutions were stored in pre-leached polyethylene bottles, or used at once for the ultratrace analysis studies. Trace metal levels for materials prepared in this manner approached 1-10 pg/ml for elements observable by ASV.

Solutions were transferred using an Eppendorf 100 µl pipette with disposable tips that had been pre-leached in an 8N solution of Ultrex HNO_3

in distilled water. All glassware was leached with 5N HNO_3 between uses, and the cell and electrodes were stored in 5N Ultrex HNO_3 between analyses.

A Beckman 4500 digital pH meter was used to measure the pH values of solutions.

Software

A variety of computer programs were written for this work. These included a program to plate either mercury or gold on the glassy carbon electrode, the main ASV program, a plotting program and a collection of routines designed to allow remote hardcopy plotting of ASV runs at the University Computing Center.

Automated Plating of the Electrode. Reproducible electrode plating conditions were assured by the use of a plating program, written in PDP-11 FORTRAN IV. The routine allows input of the parameters described in Table II, and calls a subroutine written in MACRO-11, the PDP-11 assembly language, which implements the parameters and performs the plating. Upon completion of plating, the program exits, but maintains the electrode voltage at its ending value (-31mv for Hg, and +600mv for Au, both relative to the SCE) to prevent removal of the film. Films prepared using this program were found to be reproducible to better than 1% by placing a silver coulometer in series with the cell. This program was used to generate all films used in this work.

ASV Sampling Program. This program consists of a driver routine and three subroutines written in FORTRAN IV, with four other subroutines written in MACRO-11. The main routine, the disk storage subroutine and the various libraries are core resident, while the interactive input routine, sampling routines, and filtering routines are overlayed from disk into core memory as required, since these are not all needed at once. Table III diagrams the structure of the system used.

When the program is started, subroutine SETUP gives the operator a choice of default parameters suitable for a variety of analyses, or the option of specifying the parameters for the run. These parameters are checked for errors, and passed to the driver, which swaps the appropriate sampling routine in, over SETUP.

One or more sampling runs are performed, and the run(s) are then filtered, if desired, by means of the following sequence of steps: The data are pseudorotated to obtain values of zero for the starting and end points (51), transformed into the Fourier domain, multiplied by a rectangular function that has the effect of keeping only the first 16 Fourier coefficients, then reverse-transformed to the time domain again, and finally pseudorotated back to the original aspect. This process, a Fourier transform based digital filter, is similar to one used by Betty and Horlick (52), although it multiplies both the real and imaginary parts to avoid altering the phase relations in the data (53). The net effect of this process is an effective, if somewhat severe, low-pass filter that adds no distortion to the data, unlike an analog low-pass RC filter (54). Thus, peakshape and peak width information is unaffected by the filtering process. Peaks are slightly attenuated by the filtering, but for noisy data, the improvement in signal-to-noise (S/N) ratio is substantial.

Next, the data are displayed in the form of a conventional ASV voltammogram on the TEK 4012 terminal, and the data (or the filtered data, if filtering was requested) are stored on the disk under a user-specified file name by STORIT.

At this point, a variety of events can occur, depending upon what was specified earlier. It is possible to have the program sequence through a specified number of separate ASV experiments, differing by a pre-selected

value in the plating potential. A description of this technique, and results from runs using it, are presented in another paper (55). If the above option is not selected, the program will repeat the entire experiment on command, facilitating the analysis of samples through standard additions. As many repeats can be requested as there is room on the disk; all runs are stored sequentially under the same file name for easy access. When no more repeats are desired, the program exits and closes the data file on the disk. The entire process is summarized by the flowchart in Figure 3.

Some further comment should be made on the two assembly-language routines that actually perform the ASV experiment. The routine SAMPLR, used to generate a linear scan ASV experiment, produces a waveform like that shown in Figure 4. An initial period of 30 seconds is allowed after stirring is begun, before the deposition potential, V_d, is applied and the timer started. This period is provided to allow the solution to be more reproducibly plated onto the electrode. Time is counted down, and displayed in the digital display, until 15 seconds remain, when stirring is halted, to allow the solution to become quiescent. Deposition at V_d continues until 2 seconds remain, when the potential is switched to the rest potential, V_r. The stripping scan is then initiated by loading the rate into DAC 1, and triggering the ramp generator, while also starting the sampling clock. At predetermined periods, clock overflow starts the ADC conversion, which causes an interrupt upon finishing each conversion. The interrupt is serviced and the datum is either stored, or held in an intermediate location if several data values are to be averaged to obtain a single datum, in effect causing the ADC to act as an integrating ADC, removing high frequency fluctuations in the data. This process continues until 256 points have been collected, at which time the scan is halted, and the data are processed. If multiple

scans were desired, as in the method of Kryger and Jagner (17-19), more scans like the one discussed above follow, the data being stored at the end of each scan using a normalized data averaging algorithm (56) given by the equation:

$$A_n = \frac{S_n - A_{n-1}}{n} + A_{n-1} \qquad (6)$$

where A_n is the average of the data for any given point after n scans, and S_n is the value of that point obtained during scan n.

After the completion of the analyte scan(s), the potential is switched to the cleaning potential, V_c, to remove all materials deposited, other than the electrode film itself, from the electrode. This is necessary as the ending potential for a scan may not be anodic enough to remove all other material, and a buildup of material might otherwise occur, invalidating the experiment. The timer and rotator are again started; stirring is allowed to continue for 20 seconds at the user-selected rotation rate, after which a rest time of 10 seconds is allowed for the solution to become quiescent again. With 1 second remaining, the potential is again switched to the rest potential and another scan is performed exactly analogous to the previous analyte scan. As before, multiple scans can be run, if desired. The only difference is that the data are stored in a different array.

If, during a scan any sample exceeds the capacity of the ADC, a flag is set, and a count is made of the number of times samples overflowed the ADC. If this number exceeds the number allowed by the operator, the main program reduces the system gain, if possible, and instructs the sampling program to repeat the experiment. If no further reduction in gain is possible, the main program terminates the run, and issues an explanatory message.

The staircase sampling routine, STAIRS, is similar to the linear scan routine except for the mechanics of the stripping step. The waveform is shown in Figure 5. There, the delay time, τ, is loaded into clock 1, and the sampling time is loaded into clock 2. The first potential step starts clock 1, which starts clock 2 upon underflow. Clock 2 times the interrupt-based sampling of the ADC for the datum (or for the points to be averaged to one point) and restarts clock 1 upon collecting the data for the pulse. Simultaneously, another pulse is made by suitably changing the value at DAC 1. This process continues until the number of steps corresponding to the required voltage range is performed. Here, the number of samples collected depends upon the voltage range limits selected. The subroutine SETUP calculates the step height required to maximize the number of samples, subject to the constraint that there be fewer than 257. The staircase waveform routine was also provided with the automatic overflow detection and gain reduction capability.

Remote Plotting of ASV Runs. Plotting of individual runs is performed automatically by the main program on the TEK 4012, but hard copy plots are also available via a sequence of programs that (1) convert ASV data files into strict integer format, (2) perform binary transmission of the data files to the CDC 6400 on a 1200 baud line, (3) convert the resultant octal file on the CDC to a floating point decimal file, and (4) call local Calcomp routine-based utility plotting packages (57,58) perform the plots; with the exception of the binary transmission program, these programs are written in FORTRAN.

Procedure

Preparation of the Electrode. The first step of the analysis is the preparation of the electrode for the TFME, a solution of 2×10^{-3} M

$Hg(NO_3)_2$ in 0.1M KNO_3 was used. The plating potential used was -1000mv vs the SCE, as it is claimed (59) that films plated in this potential region are homogeneous. The electrode was rotated at 3500 rpm and the solution was purged by nitrogen for 600 sec while the working electrode was held at a potential of +118 mv vs the SCE to prevent any mercury deposition. At the end of the oxygen removal time, the potential was switched to -1000mv and held there for a time suitable to generate an appropriate film thickness (250 - 300 nm). At the end of the plating time, the potential was switched to -31 mv vs the SCE to remove impurities in the Hg film, but not to remove the Hg film itself.

Film thicknesses were calculated, assuming 100% efficiency and homogeneous coverage, from the electrode area and the number of coulombs passed, as measured by a silver coulometer in series with the cell. Plating efficiencies have been found to be essentially 100% in solutions containing 2×10^{-3} M $Hg(NO_3)_2$ (21), so the above assumptions are reasonable.

For gold film electrodes, a similar procedure was employed. There, a 10^{-5} M solution of $HAuCl_4$ in 0.1 M $HClO_4$ was used without deaeration. Plating was performed for 500 seconds with a rotation rate of 3000 rpm at 0.0v vs the SCE, and the electrode was stripped of codeposited impurities by holding it at -848 mv vs the SCE for 120 seconds. This is essentially the method used by Allen (15). Adherent films of a gold-like sheen resulted from this process, in contrast to results reported for Au films on pyrolytic graphite (60), where slow deposition was recommended.

Stripping Voltammetry. Once the electrode is prepared, the cell was disconnected, the reference and counter electrodes rinsed with 3N Ultrex HNO_3 and finally distilled water, and the cell, also rinsed with HNO_3 and distilled waterwas charged with sample solution. The solutionwas purged with

nitrogen for five minutes with the RDE rotating at 1500 rpm, during which time the experimental parameters were entered into the computer. Before plating, the nitrogen stream was diverted over the solution and the rotation of the RDE was halted to avoid entrapment of bubbles on the electrode. The ASV experiment was then allowed to proceed automatically. Multiple standard additions were used to quantitate species.

RESULTS AND DISCUSSION

Effects of Hg Film Thickness on System Response

In order to determine the optimal Hg film thickness for analyses of the metals Zn, Pb, Cd and Cu, the usual ones analyzed by ASV techniques, a 75 ml solution of 0.1M acetate buffer (pH = 5.62) containing a spike of Cu, Zn, Pb, and Cd so that concentrations of the metals was 1 ng/ml in each case, was analyzed by linear scan ASV with the background correction. A single scan, using a 16-point average was used to analyze the solution. Hg film thicknesses of 50 nm to 350 nm were used, and at least four runs were performed for each film thickness, with only the average results being reported here. Figure 6 summarizes the results found. From the figure, it is clear that, for Hg films above 150 nm in thickness, the response is essentially constant, except in the case of Cu, which shows an optimum response with Hg films having thicknesses between 200 and 250 nm. Zn gave non-reproducible values at very thin Hg films, and these are not plotted. These results agree with those of Pinchin and Newham (61) fairly well, although those authors found increased sensitivity for Cu when very thin Hg films were employed.

In view of the above results, Hg films of 250 nm were used throughout the remainder of the study with excellent results.

Effects of Deposition Time

The effects of varying deposition time on the peak heights of Pb, Cd and Zn were investigated. By Faraday's law:

$$C_R^o = \frac{it}{nFA\ell} \tag{7}$$

where t is the deposition time and i is the reduction current of the metal in question. For the RDE, i can be calculated from equation 5. Upon combining equations 1, 5, and 7, the following equation is obtained:

$$i_p = 0.88\ \pi^{1/2}\ \frac{n^2F^2}{eRT}\ D_{ox}^{2/3}\rho^{-1/6}\ \omega^{1/2}\ A\nu t\ C_{ox}^o \tag{8}$$

This equation indicates a linear relation between deposition time and peak height.

A 75 ml solution of 0.01 M acetate buffer, containing 1.66 ng/ml Pb, 4.33 ng/ml Cd and 0.80 ng/ml Zn (as determined by subsequent analysis of the solution) was examined, and results are plotted in Figure 7. These results indicate from examination of slopes that the technique is more sensitive to Cd than Pb or Zn, and that a straight line relation is observed, at least for the concentrations studied. Similar results have been obtained for conventional ASV (62).

Effects of Scan Rate

According to both the exact theory of linear scan ASV (30,31), the approximate theory given by equation 8, and the Ševčik-Randles theory (35,36), peak heights should be linearly related to the scan rate. Peak widths should also increase with increasing scan rate, up to the limit of 101 mv predicted by Ševčik and Randles.

The same solution used for the deposition studies was used to study the effects of scan rate. Again, a linear relation was obtained in all cases, as can be seen from examination of Figure 8, which plots scan rate versus peak

height. Peak width also increased, as can be seen from an examination of Table IV, where peak widths of the Cd stripping peak are listed as a function of the scan rate; the maximum value observed, 100mv, is in excellent agreement with the value predicted by theory. This agreement indicates the adequacy of equation 8 for rates up to 3500 mv/sec, as system response is not noticeably degraded. Because of these results, scan rates of from 2500 - 3000 mv/sec were used in later studies of ultratrace solutions to gain the maximum signal possible.

Effects of Electrode Rotation

Equation 3 predicts a linear relation between the square root of the electrode rotation rate and the amount of material deposited on the electrode, which, since the amount of material deposited should be directly proportioned to the peak height, as shown by equation 8, predicts a linear relation between $\omega^{1/2}$ and peak height.

Figure 9 illustrates the relation found. Above 6500 rpm, turbulence was observed in the solution, and bubbles were noticed at the electrode. Stripping currents were severely depressed as a result; rotations above 6500 rpm were thus not accessible with the cell design used here. Again, good linearity was observed, and equation 8 is found to hold.

Rotation rates of between 3000 and 4000 rpm were used in this work to avoid turbulence, but still maintain reasonable sensitivities.

Peak Position as a Function of Scan Rate

Equation 2 predicts a logarithmic relation between scan rate and the shift in the peak potential for any given peak. That is:

$$E_p = E^{o'} + 2.3 \frac{RT}{nF} \log \frac{nF\delta\ell}{RTD_{ox}} + \frac{2.3\ RT}{nF} \log\nu \qquad (9)$$

The effects of varying scan rate on the peak potential for Pb, Cd, and Zn were investigated, and results are plotted in Figure 10. Since the three metals

examined are capable of transferring 2 el4ctrons, slopes of 29.5 mv should have resulted. In fact, the slopes are considerably higher, about 65 mv. Thus, the shifts are more than predicted by theory, which can be the result of several factors. One possible cause is uncompensated resistance between reference and working electrodes, since potential shifts can (and will) result from any uncompensated resistance in the solution. Since, as has already been established, larger currents result from rapid scan rates, the IR drop associated with any given scan rate also increases linearly with scar rate, having the effect of causing an additional potential shift to the peak in an anodic direction. Since the IR drop responds both to capacitive as well as faradaic current, even a small uncompensated resistance can lead to shifts on the order of those observed.

A second possible cause of the discrepancy is the assumption implicit in equation 8 of a constant diffusion layer δ, despite the fact that the scan rate is increased by a factor of about 250 through the runs. Since the peak potential depends linearly on δ as well as ν, the scan rate, changes in δ with ν will give anomalously high values for the slope of a plot of Ep versus log ν. This is exactly the situation observed here.

A third factor for the discrepancy is the assumption of thin films and slow scan rates in the derivation of equation 2 (32). Since the scan rates used in this study are by no means slow, there is no certainty that the theory should hold exactly.

It is likely that IR drop as well as a changing diffusion layer thickness contribute to the error observed. No special effort was made in this work to optimize the cell geometry to minimize the IR drop, nor was positive feedback IR compensation employed (45) in these studies, and thus some small uncompensated resistance is likely in the 0.1 M supporting electrolyte used.

If we assume a 10Ω resistance, a full scale (150 μamp) current gives rise to an error of 1.5 mv in the potential applied to the electrode; the shifts observed are on this order for slower scan rates. Since shifts of much greater magnitude are observed for the faster scan rates, changes in the diffusion layer must also be suspected. Errors here would be small at slow scan rates, but larger at the higher scan rates.

System Response to Metal Concentration

Since the basis of analysis using the ASV technique is the method of standard additions, a determination of the effects of varying the metal concentration must be performed. Equation 8 predicts a linear response, and this response has been verified many times (for example (62)) in conventional ASV.

A variety of solutions were examined, using various experimental conditions; except where noted below, all gave a linear response to added metal concentration. Only examples will be given here.

Linearity of response in the lower ng/ml range is shown in Figure 11. The metal used here is Cd, with only a 60 second deposition time. Each point is the average of 2-3 determinations.

Response was also linear in the sub-ng/ml range. A carefully purified 0.1 M acetate buffer was used for the simultaneous determination of ultra-trace levels of Cd and Pb. Plating at -800mv (SCE) for 300 seconds, followed by a single, rapid scan from -800 to -10mv (SCE) produced reasonable peaks. Figure 12 shows the determination of Cd on one such solution, and Figure 13 shows the plot for the simultaneous determination; there, increments of 7 pg/ml were used to quantitate the buffer. As can be seen from the two slopes, the system is slightly more sensitive to Cd than Pb at pg/ml levels. Zn was not examined, as pure buffers (pg/ml) could not be obtained with respect to this element.

For similar concentrations of Cu, system response is also linear, but other factors also appear. A carefully purified 0.1M KCl buffer was used to quantitate Cu at pg/ml levels. A 300 sec deposition at -600mv (SCE), followed by a single, rapid scan to 0 mv (SCE) was used, and reasonable peaks resulted. Peak quality and S/N ratio was not as good as for the Cd and Pb run, however. Figure 14 shows the graph of the standard addition of 5 pg/ml Cu to the solution, and Table V lists the peak half width for the runs, for which a 200 nm Hg film was used. A Cu concentration of 18 pg/ml was determined by standard additions.

The constancy of the peak width and the symmetric peak shape suggest that no unusual effects, such as those observed by Pinchin and Newham (62), occur in this case. The peak with (90 mv) was consistent with widths observed at similar scan rates (900 mv/sec). Some broadening of the peak for Cu is indicated, as has been observed by Florence and Batley (63) in chloride solutions containing Cu. Upon increasing the total Cu concentration beyond about 50 pg/ml, deviations from linearity resulted. For much larger Cu concentrations, on the order of ng/ml, peak shapes deteriorated substantially in chloride buffer, as observed by Pinchin and Newham (61). In this case determinations of Cu in acetate buffer are superior. A comparison of the slopes of Figures 13 and 14 indicates the lower sensitivity of ASV for Cu in chloride solution, as observed by Florence and Batley (77).

Thus system response is generally linear for metal concentration, and again equation 8 is seen to hold.

System Reproducibility and Sensitivity

A variety of samples were analyzed to evaluate the reproducibility of the technique. Typical results are reported in Table VI. Reproducibilities of 1 - 2% are readily obtainable for concentrations in the ng/ml range,

while only slightly poorer reproducibilities (4-5%) are obtained at the pg/ml level. These results, run on the same film, are comparable with the published results from other computer-controlled ASV instrumentation (21,27), but they are substantially better for the pg/ml reproducibilities previously reported (64), where values vary by 20-30%, primarily due to long (30 minute) deposition times.

Another factor invovled with reproducibility is the system signal-to-noise level. It was observed that the noise was largely constant for a given supporting electrolyte concentration and gain range. For a supporting electrolyte of 0.1M KNO_3 and a full scale range of 144 μamp, the standard deviation of the noise was observed to be about 0.6 μamps. This is a relatively large noise level, and was the reason for using point averaging and filtering techniques to increase the S/N ratio. Using a 16 point average, the noise can be theoretically reduced to 0.15 μamp, a more acceptable level for this type of work. With this noise level, noise-related fluctuations in the peak heights for all but the most dilute (pg/ml) solutions become relatively unimportant, in view of the variation of the value of the diffusion constant with temperature, about 1% deg^{-1} in most cases (65). Since the cell was not thermostatted, this uncertainty became dominant in the determination of peak heights.

Using the 0.15 μamp value for noise, an approximate detection limit may be calculated, ignoring peak height errors due to temperature for the moment. The slopes of the calibration lines for Cd, Pb and Cu are given along with 4σ noise levels in Table VII. Detection limits on the order of 1 pg/ml are achievable by the method. Inclusion of the 1% relative error of the diffusion constant will slightly increase these limits.

Other contributions to the overall error are not as important, as an analysis of error (66) using equation 8 shows. Taking the total derivative of equation 8, and allowing the errors to be finite:

$$\Delta i_p^2 = \left(\frac{\partial i_p}{\partial D}\right)^2 \Delta D^2 + \left(\frac{\partial i_p}{\partial p}\right)^2 \Delta p^2 + \left(\frac{\partial i_p}{\partial \omega}\right)^2 \Delta \omega^2 + \left(\frac{\partial i_p}{\partial \nu}\right)^2 \Delta \nu^2 + \left(\frac{\partial i_p}{\partial t}\right)^2 \Delta t^2 + \left(\frac{\partial i_p}{\partial T}\right)^2 \Delta T^2 \qquad (10)$$

Equation 10 estimates the total random error in the peak current due to random error in the measurable parameters. Estimates of the relative errors in these parameters, as well as typical values, are given in Table VIII. Evaluation of equation 10 shows that the fluctuations in viscosity, temperature and diffusion coefficient dominate the error. A 3.7% relative error is calculated for i_p by equation 10. This error is in good agreement with errors observed using the technique here.

Staircase ASV Parameters

The effects of varying the delay time τ was investigated using background corrected ASV. Equation 3 predicts a linear relationship between τ^{-1} and i_p, which has been confirmed for conventional staircase ASV (21). For delay times less that 10 msec, this relation was observed as shown in Table IX. In general, sensitivities using background subtracted staircase ASV were far less than those observed for linear scan ASV. Baselines generated by the staircase waveform were only slightly better, and peak widths were similar to slow linear scan ASV. In view of the differences in sensitivity, staircase ASV was not studied for very dilute solutions. In more concentrated solutions, staircase ASV produced good calibration curves and clean voltammograms.

Multiple Scanning Parameters

The use of multiple stripping scans (17-19) was briefly investigated. Small word size made it infeasible to sum many scans without normalizing, as only a maximum of 16 can be summed, so the method described by equation 6 was used. As many scans as desired could then be summed.

Results from using this technique were adequate, but the method was far slower and less able to remove noise than the point averaging algorithm used for most of this work. A brief consideration of the multiple scanning process shows why the S/N suffers. If one considers a single scan of signal S and noise level A, then the signal-to-noise ratio σ is given directly by the equation

$$\sigma_s = S/A \tag{11}$$

Suppose now N multiple scans are taken, and further suppose that 90% of the material stripped on one scan returns for the next, the rest being lost to diffusion. Now the signal-to-noise ratio is given by the equation:

$$\sigma_m = \frac{\frac{S}{N}\sum_{i=1}^{N}(.9)^{i-1}}{\frac{A}{\sqrt{N}}} \tag{12}$$

allowing for normalized averaging on N runs to reduce the noise by N. Since the product of the sum with the quantity $\sqrt{N}/N$ is less than 1, $\sigma_m < \sigma_s$. Even allowing 99% return does not change the result. Examination of the voltammograms in reference 18 suggests that a value of 80% return is more reasonable, giving a $\sigma_m = 0.79\sigma_s$. Because of this undesirable feature, this method was not used after comparative runs on dilute solutions confirmed the theoretical predictions above, in that normalized multiple scan signals were observed to be about 0.8 as intense as the averaged point signals.

Effectiveness of Background Compensation

The effectiveness of background compensation was investigated by analyzing Zn in acid solutions. Normal analysis for Zn in these solutions is difficult, due to the effects of the evolution at the electrode (67). Table X lists the results of Zn determinations in pH 6.6 and 2.0 solutions. Although the sensitivity of the determination is degraded, analysis for Zn in acidic solutions is still quite straightforward. These results, and the results for copper discussed earlier, indicate that the digital background subtraction technique performs effective compensation of the capacitive and background currents. Total compensation is not achieved, as the activity of the film changes slightly, but sensitivities and precision are still quite adequate, in contrast to some claims (68).

CONCLUSIONS

The work reported above has demonstrated the feasibility of using a rapid linear scan-based ASV experiment, coupled with digital background subtraction, for routine analyses.

Results consistent with theory were observed for studies considering the effects of scan rate electrode rotation, deposition time and added metal.

In summary, rapid-scan, background-corrected linear scan ASV appears to be one of the best ultratrace and trace analysis methods available. The combination of sensitivity, precision, and speed are at least comparable, if not superior, to all existing techniques available.

CREDIT

This work was partially supported by the Office of Naval Research. SDB gratefully acknowledges the support during the 1977-78 year of an American Chemical Society Analytical Division Fellowship, sponsored by the Perkin-Elmer Corporation.

REFERENCES

1. S. H. Liberman and A. Zirino, Anal. Chem., 46, 20 (1974).
2. J. Wang and M. Ariel, J. Electroanal. Chem., 83, 217 (1977).
3. J. Wang and M. Ariel, J. Electroanal. Chem., 85, 289 (1977).
4. W. R. Matson, D. K. Roe and D. F. Carritt, Anal. Chem., 37, 1594 (1965).
5. E. P. Parry and R. A. Osteryoung, Anal. Chem., 37, 1634 (1965).
6. G. Barker and A. W. Gardner, Z. Anal. Chem., 173, 79, (1960).
7. J. B. Flato, Anal. Chem., 44, 75A (1972).
8. H. Sigerman and G. O'Dom, Amer. Lab., 4 (6), 59 (1972).
9. G. D. Christian, J. Electroanal. Chem., 23, 1 (1969).
10. T. R. Copeland, J. H. Christie, R. A. Osteryoung and R. K. Skogerboe, Anal. Chem., 45, 2171 (1973).
11. P. Valenta, H. Rutzil, H. W. Nürnberg and M. Stoeppler, Z. Anal. Chem., 285, 25 (1977).
12. T. M. Florence, J. Electroanal. Chem., 27, 273 (1970).
13. T. M. Florence, J. Electroanal. Chem., 35, 237 (1972).
14. A. H. Miguel and C. M. Jankowski, Anal. Chem., 46, 1832 (1974).
15. R. E. Allen, Dissertation, Iowa State University, 1974).
16. R. E. Allen and D. C. Johnson, Talanta, 20, 305 (1973).
17. L. Kryger, D. Jagner and H. J. Skov, Anal. Chim. Acta, 78, 241 (1975).
18. L. Kryger and D. Jagner, Anal. Chim. Acta, 78, 251 (1975).
19. D. Jagner and L. Kryger, Anal. Chim. Acta, 80, 255 (1975).
20. A. M. Bond and B. S. Grabarić, Anal. Chim. Acta, 88, 227 (1977).
21. U. Eisner, J. A. Turner and R. A. Osteryoung, Anal. Chem., 48, 1603 (1976).
22. J. A. Turner, U. Eisner and R. A. Osteryoung, Anal. Chim. Acta, 90, 25 (1977).

23. A. Zirino and M. Healy, Env. Sci. Tech., 6, 243 (1972).

24. L. Sipos, P. Valenta, H. W. Nürnberg and M. Branica, J. Electroanal. Chem., 77, 263 (1977).

25. L. Sipos, S. Kozar, I. Kontusim and M. Branica, J. Electroanal. Chem., 87, 347 (1978).

26. E. Steeman, E. Temmerman and R. Verbennen, Anal. Chim. Acta, 96, 177 (1978).

27. A. M. Bond and B. S. Grabarić, Anal. Chem., 48, 1624 (1976).

28. Q. V. Thomas, L. Kryger and S. P. Perone, Anal. Chem., 48, 761 (1976).

29. W. T. DeVries and E. van Dalen, J. Electroanal. Chem., 8, 366 (1964).

30. W. T. DeVries, J. Electroanal. Chem., 9, 448 (1965).

31. W. T. DeVries and E. Van Dalen, J. Electroanal. Chem., 14, 315 (1967).

32. D. K. Roe and J. E. A. Toni, Anal. Chem., 37, 1503 (1965).

33. J. H. Christie and R. A. Osteryoung, Anal. Chem., 48, 869 (1976).

34. R. A. Osteryoung and J. H. Christie, Anal. Chem., 46, 351 (1974).

35. J. E. B. Randles, Trans. Faraday Soc., 44, 327 (1948).

36. A. Ševčik, Coll. Czech. Chem. Comm., 13, 349 (1948).

37. S. P. Perone and J. R. Birk, Anal. Chem., 37, 9 (1965).

38. V. E. Levich, "Physiochemical Hydrodynamics,: Prentice-Hall, Englewood Cliffs, N. J., 1962.

39. J. D. S. Danielson, S. D. Brown, C. J. Appellof and B. R. Kowalski, ONR Technical Report, 1978.

40. PDP-11 Processor Handbook, Digital Equipment Corporation, Maynard, Mass., 1973.

41. PDP-11 RT-11 System Reference Manual, Digital Equipment Corporation, Maynard, Mass., 1977.

42. G. L. Booman and W. B. Holbrook, Anal. Chem., 35, 1793 (1963).

43. W. W. Schwartz and I. Shain, Anal. Chem., 35, 1770 (1963).

44. G. L. Booman and W. B. Holbrook, Anal. Chem., 37, 795 (1965).

45. R. R. Schroeder and I. Shain, Chem. Instrum., 1, 233 (1969).

46. RCA Linear Circuits and CMOS Handbooks, Camden, N. J., 1976.

47. D. E. Robertson, in "Ultrapurity: Methods and Techniques," M. Zief and R. Speights, ed., p. 207, Dekker, New York, N. Y., 1972.

48. M. Zief and J. W. Mitchell, "Contamination Control in Trace Metal Analysis," Wiley, New York, N. Y., 1976.

49. J. R. Moody and R. M. Lindstrom, Anal. Chem., 49, 2264 (1977).

50. R. W. Dabeka, A. Mykytiuk, S. S. Berman and D. S. Russell, Anal. Chem., 48, 1203 (1976).

51. Q. V. Thomas and S. P. Perone, Anal. Chem., 49, 1369 (1977).

52. K. R. Betty and G. Horlick, App. Spectros., 30, 23 (1976).

53. J. W. Hayes, D. E. Glover, D. E. Smith and M. W. Overton, Anal. Chem., 45, 277 (1973).

54. P. D. Willson and T. H. Edwards, App. Spectros. Reviews, 12, 1 (1976).

55. S. D. Brown and B. R. Kowalski, submitted to Anal. Chem.

56. J. W. Cooper, "The Minicomputer in the Laboratory, with Examples Using the PDP-11," Wiley-Interscience, New York,N. Y. 1977.

57. University of Washington Academic Computer Center, "Simplot," Revision 4, 1976.

58. University of Washington Academic Computer Center, "Numerical Plotting System," 1976.

59. M. Stulikova, J. Electroanal. Chem., 48, 33 (1973).

60. P. H. Davis, G. R. Dulude, R. M. Griffin, and W. R. Matson, Anal. Chem. 50, 137 (1978).

61. M. J. Pinchin and J. Newham, Anal. Chim. Acta, 90, 91 (1977).

62. W. Lund and M. Salberg, Anal. Chim. Acta, 76, 131 (1975).

63. T. M. Florence and G. E. Batley, J. Electroanal. Chem., 75, 791 (1977).

64. H. W. Nürnberg, P. Valenta, L. Mart, B. Raspor and L. Sipos, Z. Anal. Chem., 282, 357 (1976).

65. E. Barendrecht, in "Electroanalytical Chemistry," A. J. Bard, ed., Vol. 2, p. 53, Dekker, New York, N. Y., 1967.

66. J. Topping, "Errors of Observation and Their Treatment," Chapman and Hall, London, 1962.

67. H. Blutstein and A. M. Bond, Anal. Chem., 48, 759 (1976).

68. W. R. Matson, E. Zink and R. Vitukevitch, Amer. Lab., 9 (7), 59 (1977).

TABLE I

COMPUTER CONTROLLABLE CURRENT RANGES
FOR VOLTAMMETRIC STUDIES

Gain Range	Feedback Resistor (ohms)	Full scale Current (μamp)
0	24.9K	200
1	34.8K	144
2	44.9K	100
3	100.K	50

TABLE VI

ADJUSTABLE PARAMETERS FOR AUTOMATED PLATING
FOR RDE

Parameter	Function	Values Allowed
EPLATE	Set deposition potential	-2.5 to + 2.5 v
ETIME	Set deposition time	0 - 4000 sec
EROT	Set rotation speed for deposition	0 - 10000 rpm
OTIME	Set deaeration time	0 - 4000 sec
FILM	Select type of film	Au, Hg

TABLE III

ASV DATA ACQUISITION PROGRAM STRUCTURE

Segment	Type	Language[a]	Function
VOLTA	core resident	F	driver, plot driver, control
STORIT	core resident	F	disk storage of data
SETUP	overlay	F	input run parameters, error checking
FILTER	overlay	F	drives Fourier Transform filter for noisy data
SAMPLR	overlay	A	performs linear scan ASV expt.
STAIRS	overlay	A	performs staircase ASV expt.
FFTSC	overlay	A	performs fast Fourier transform
IQSIN4	overlay	A	supplies transcendental function values to FFTSC
PLTLIB	core resident	F, A	performs Calcomp plots on TEK 4012 screen

[a] Languages are: F - FORTRAN IV
A - MACRO - 11

TABLE IV

EFFECTS OF SCAN RATE ON Cd PEAK HALFWIDTH

Scan rate (mv/sec)	Cd peak height (μa)	Cd peak width[a] (mv)
3333	108	100
2850	95	100
2000	69	92
1330	50	88
1000	40	80
800	33	78
667	29	78
572	25	78
500	23	77
333	18	76
250	13	75
200	10.7	68
166	9.1	68
143	8.0	66

[a] measured at half-height.

TABLE V

PEAK WIDTH OF Cu STRIPPING PEAKS
AT ULTRATRACE LEVELS

Cu Concentration (pg/ml)	Peak Halfwidth[a] (mv)
18	94
23	90
28	90
33	90
38	94
43	90
48	91
53	90
58	90
63	90

[a] measured width at half-height.

TABLE VI

REPRODUCIBILITY OF PEAK HEIGHTS

Element	Concentration (pg/ml)	Peak Height (μamp)
Cd	32	8.6
	32	8.9
	32	9.0
Zn	20000	33.3
	20000	33.7
	20000	34.3
Zn	4000	11.2
	4000	11.4
	4000	11.3
Pb	22	4.8
	22	5.0
	22	4.9
	22	4.9

TABLE VII

SENSITIVITY AND APPROXIMATE DETECTION LIMITS
OF Cd, Pb and Cu by ASV

Element	Slope (μamp-ml/pg)	4σ detection limit (pg/ml)
Cd	1.11	0.54
Pb	0.85	0.71
Cu	0.29	2.1

TABLE VIII

RELATIVE ERRORS IN PARAMETERS RELATED TO PEAK CURRENT

Parameter	Typical Value	Estimated Relative Error
D	2×10^{-5}	1%
ρ	1×10^{-2} gm/sec/cm	0.1%
ω	4000 rpm	0.1%
ν	2500 mv/sec	0.1%
t	300 sec	0.01%
T	296 K	0.4%

TABLE IX

EFFECTS OF THE DELAY TIME ON
PEAK HEIGHT

Delay Time (msec)	Peak Height[a] (μamp)
1	100
2	102
4	104
8	108

[a] 20 ppb Cd in 0.1 KNO_3; ΔE was 4.88 mv.

TABLE X

ANALYSIS OF Zn IN ACIDIC SOLUTION

pH	Zn peak height (μamp)	Zn found (ng/ml)
6.6[a]	32.3	21.0
6.6	33.7	21.9
6.6	34.1	22.2
2.0[b]	13.8	22.1
2.0	14.8	23.6
2.0	14.9	23.8

[a] Solution was 22 ppb Zn in 0.1 M KNO_3.

[b] Solution was 22 ppb Zn in 0.1 M KNO_3 - 0.01 M $HClO_4$.

CAPTIONS FOR FIGURES

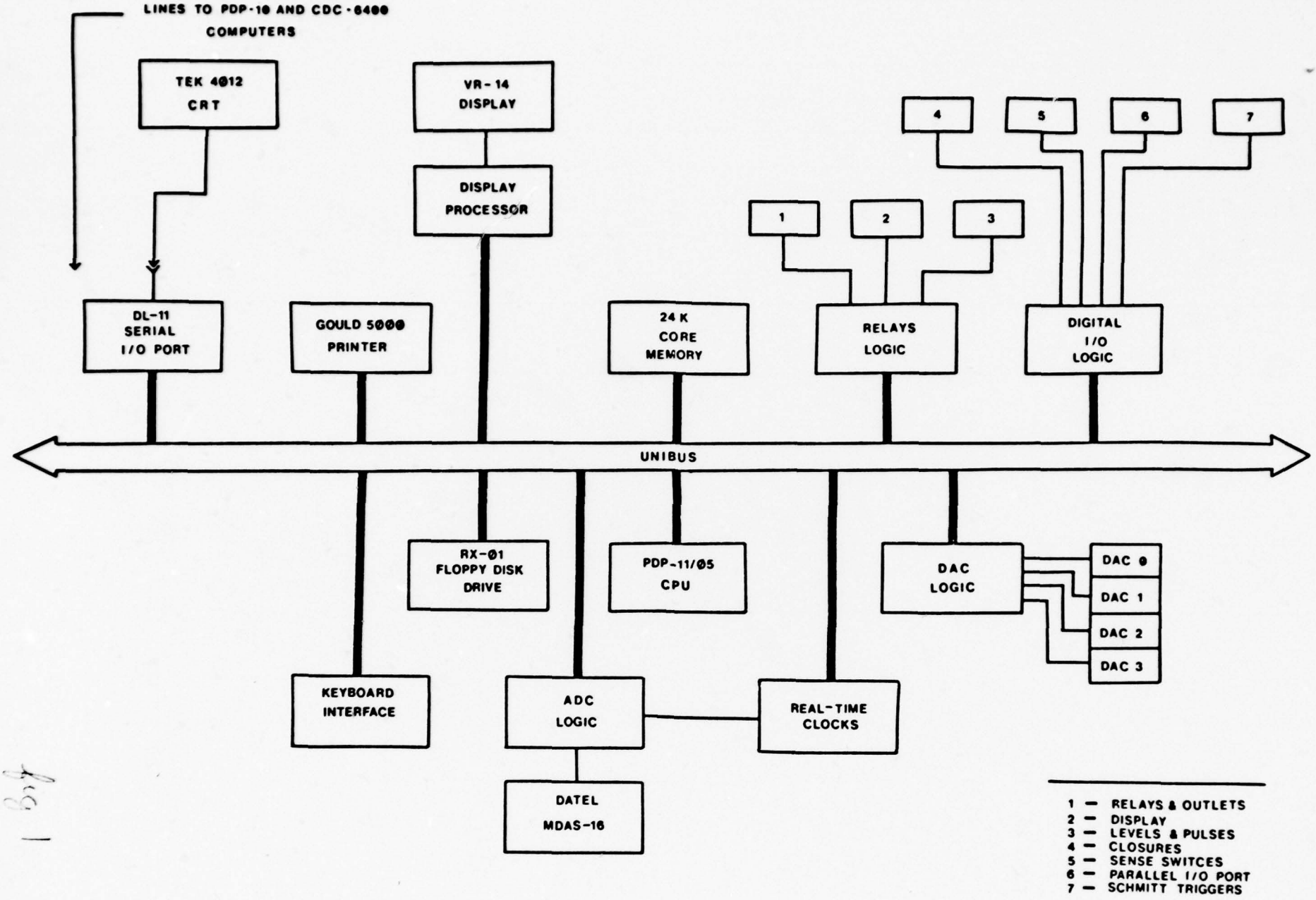
LINES TO PDP-10 AND CDC-6400 COMPUTERS
TEK 4012 CRT
VR-14 DISPLAY
DISPLAY PROCESSOR
4
5
6
7
1
2
3
DL-11 SERIAL I/O PORT
GOULD 5000 PRINTER
24 K CORE MEMORY
RELAYS LOGIC
DIGITAL I/O LOGIC
UNIBUS
RX-01 FLOPPY DISK DRIVE
PDP-11/05 CPU
DAC LOGIC
DAC 0
DAC 1
DAC 2
DAC 3
KEYBOARD INTERFACE
ADC LOGIC
REAL-TIME CLOCKS
DATEL MDAS-16
1 — RELAYS & OUTLETS
2 — DISPLAY
3 — LEVELS & PULSES
4 — CLOSURES
5 — SENSE SWITCES
6 — PARALLEL I/O PORT
7 — SCHMITT TRIGGERS

1 Box

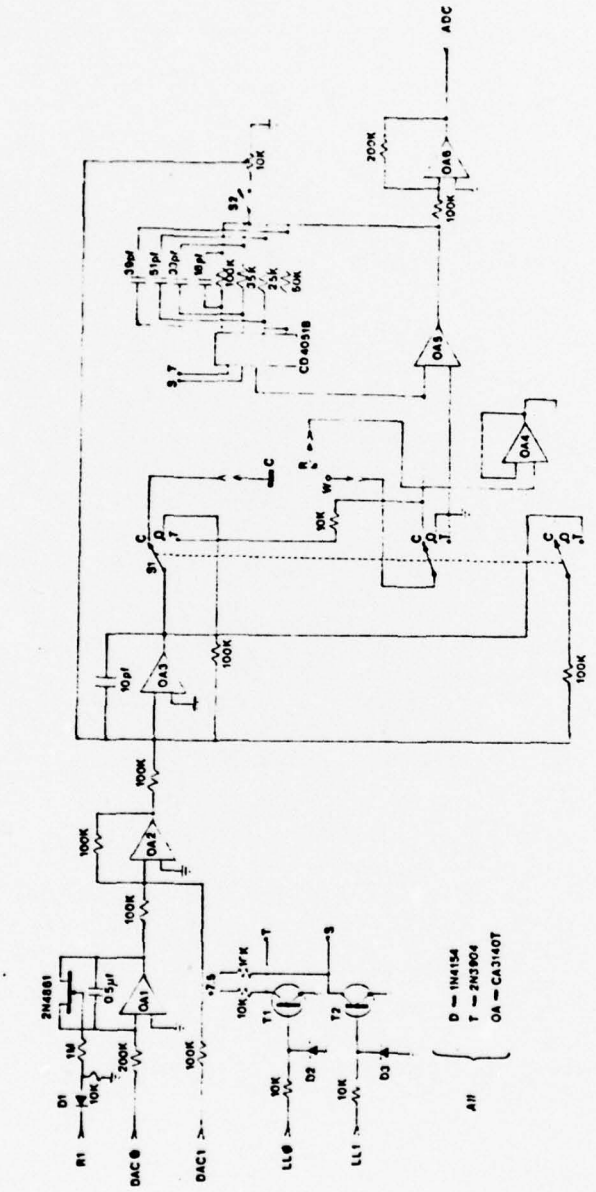
ADC
200K
OA5
100K
S2
10K
39pf
51pf
33pf
18pf
100K
35K
25K
10K
CD4051B
OA3
OA4
C
R
W
10K
S1
10pf
OA3
100K
100K
100K
OA2
100K
OA1
2N4861
0.5μf
1M
10K
200K
100K
D1
R1
DAC 0
DAC 1
10K
T1
T2
10K
D2
10K
D3
LL0
LL1
All
D — 1N4154
T — 2N3904
OA — CA3140T

Figure 2

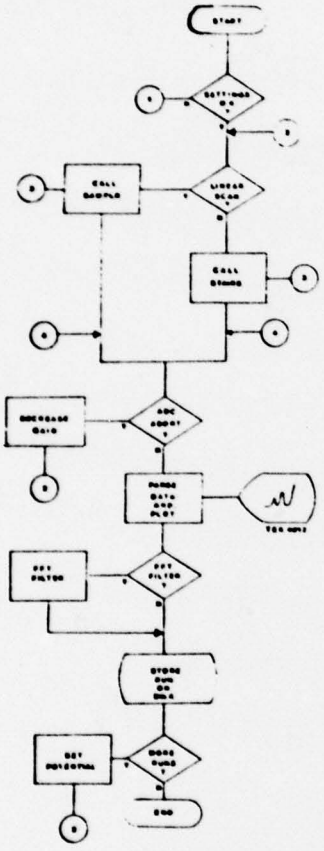

DRIVER ROUTINE

I/O ROUTINE

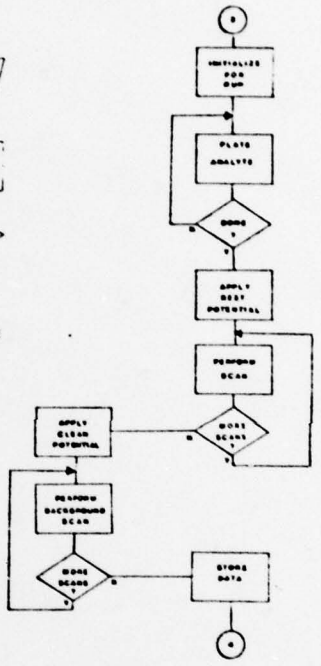

SAMPLING ROUTINES

Figure 3

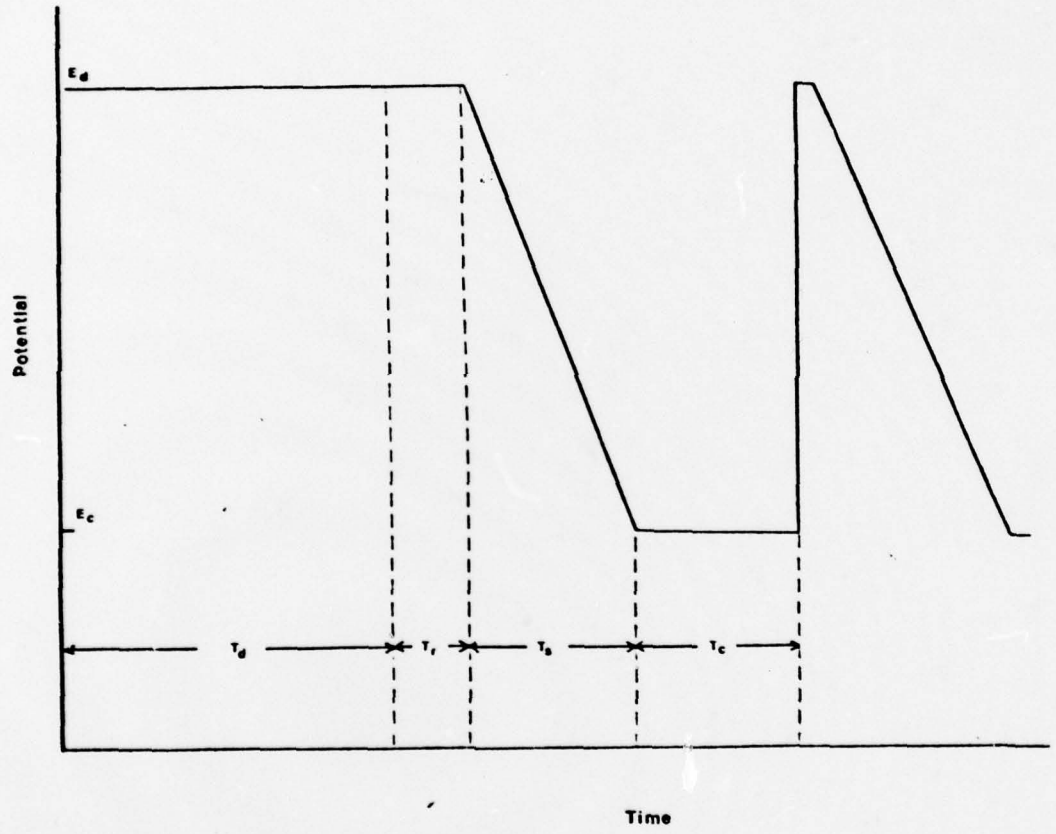

Figure 4

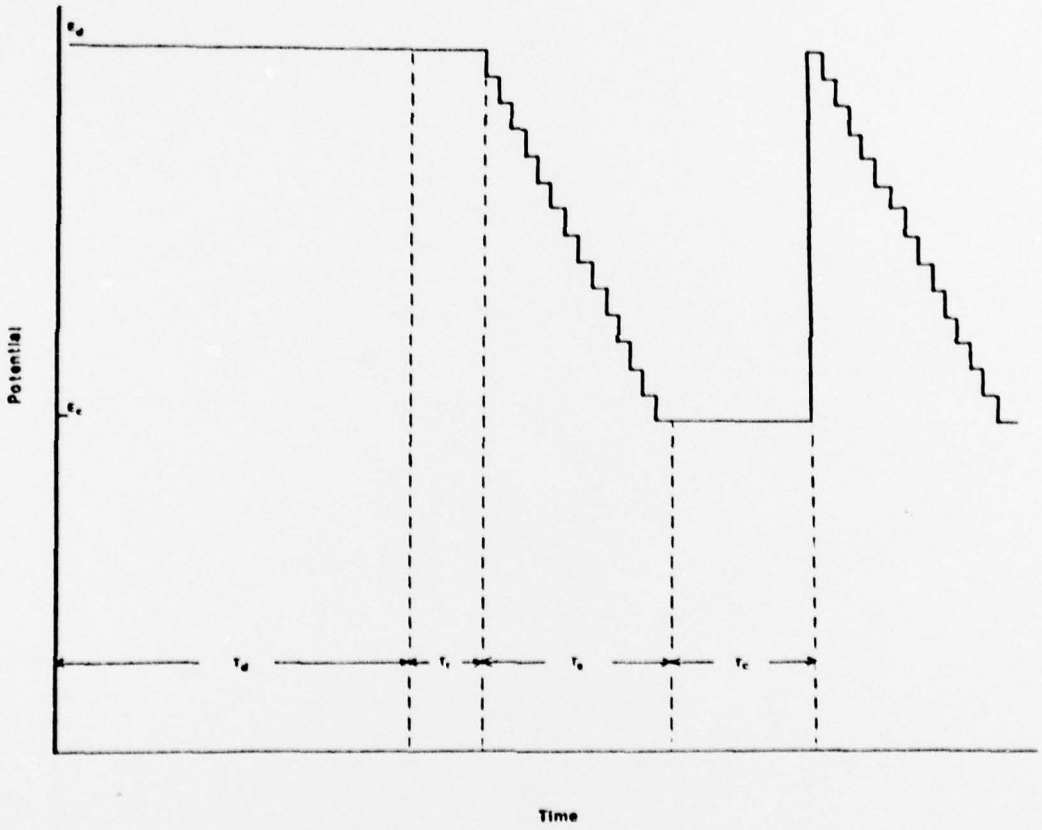
Potential
Time

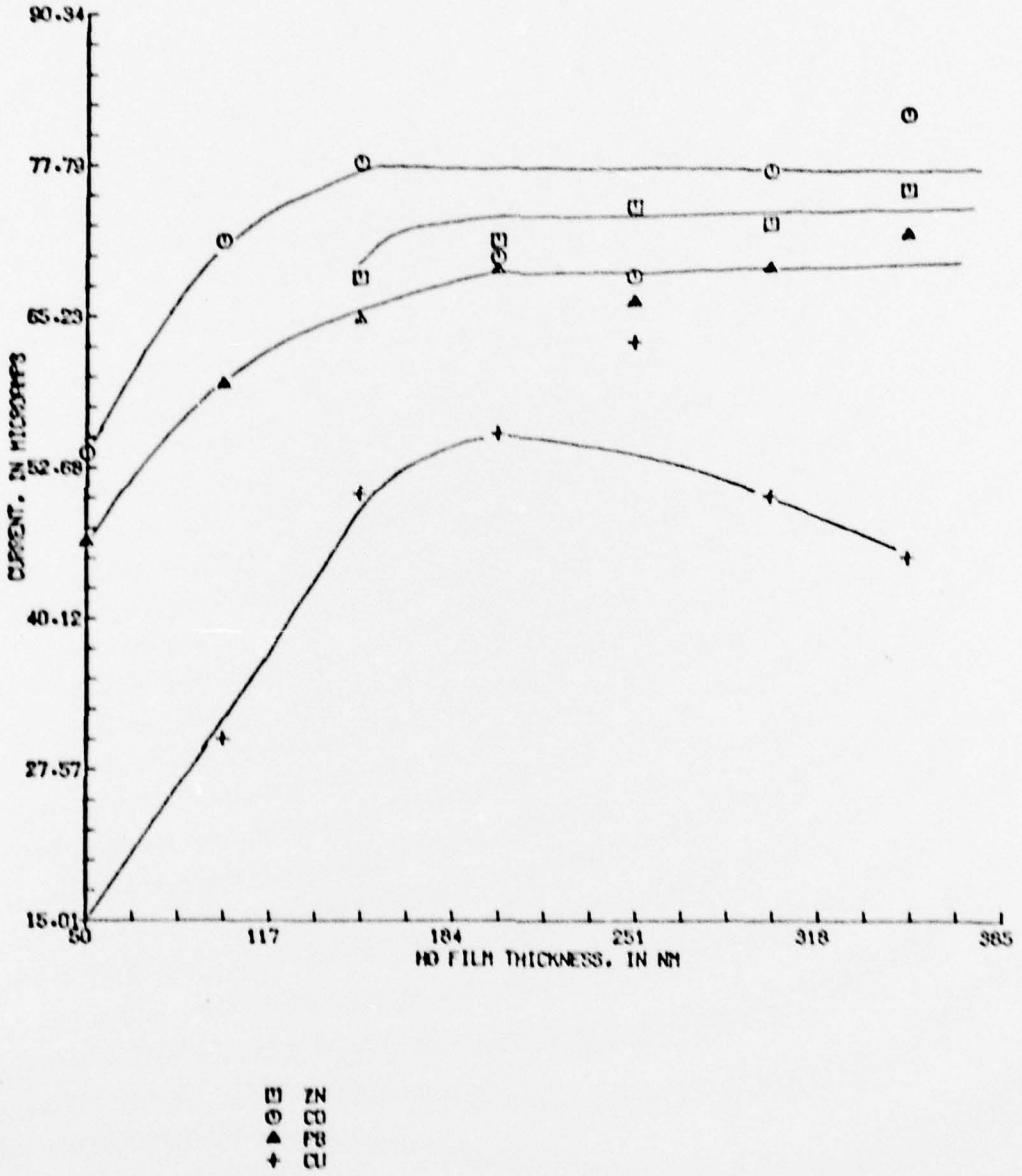
90.34
77.79
65.23
52.68
40.12
27.57
15.01
CURRENT, IN MICROAMPS
50
117
184
251
318
385
MO FILM THICKNESS, IN NM
NI
CO
FE
CU

Figure 6

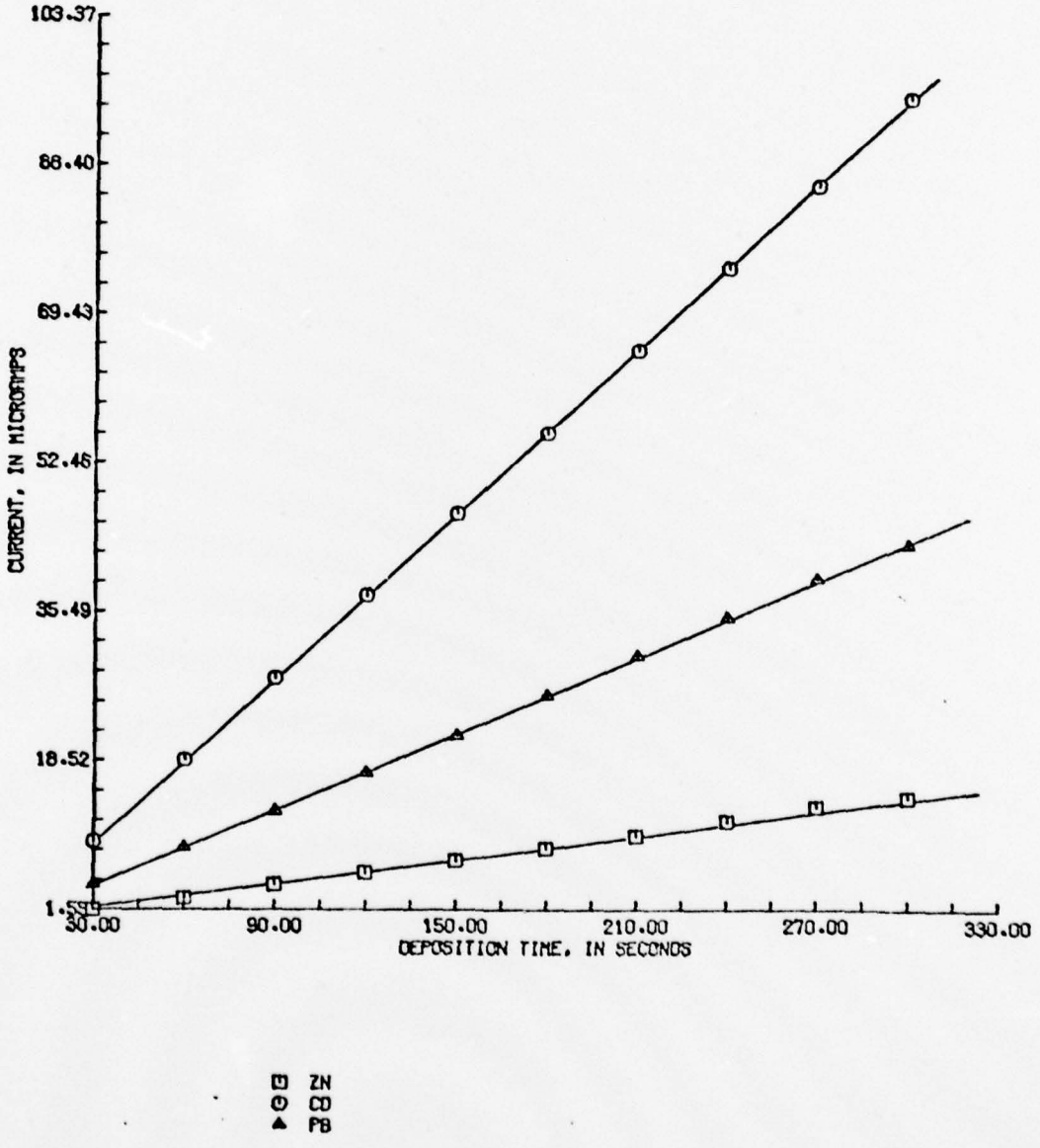
103.37
86.40
69.43
52.46
35.49
18.52
1.55
CURRENT, IN MICROAMPS
30.00
90.00
150.00
210.00
270.00
330.00
DEPOSITION TIME, IN SECONDS
ZN
CD
PB

Figure 7

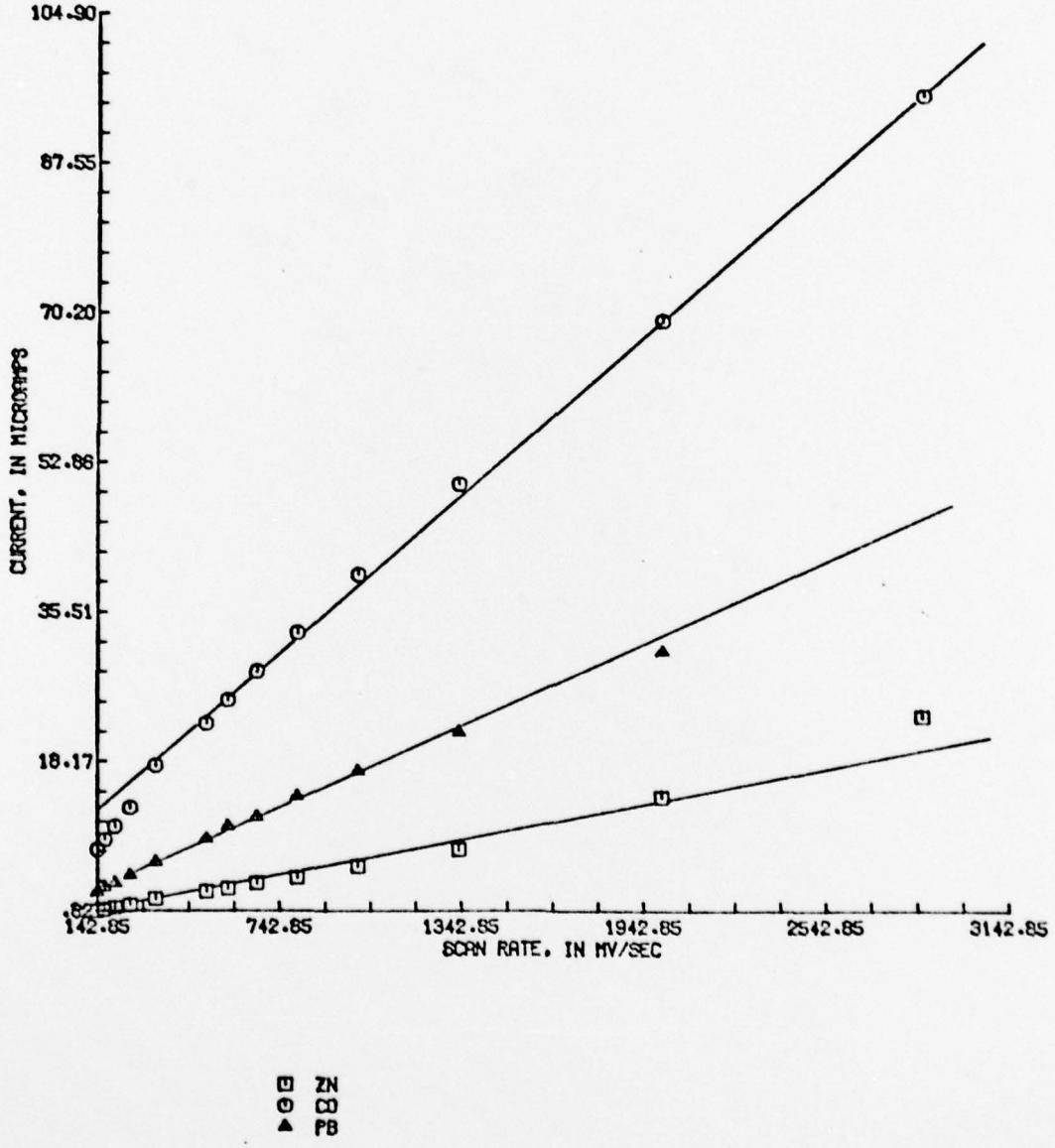
104.90
87.55
70.20
52.86
35.51
18.17
.82
CURRENT, IN MICROAMPS
142.85
742.85
1342.85
1942.85
2542.85
3142.85
SCAN RATE, IN MV/SEC
ZN
CD
PB

Figure 8

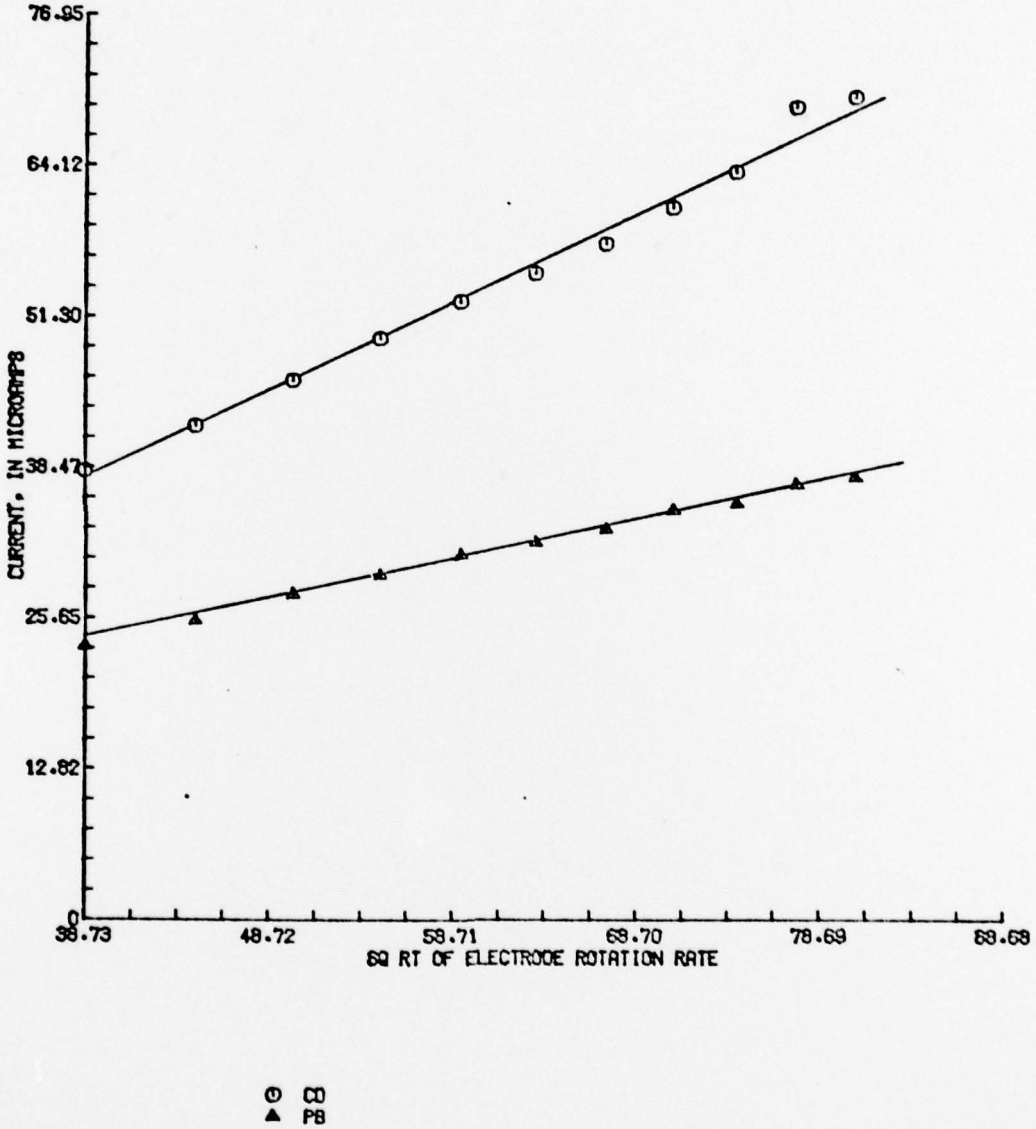
76.95
64.12
51.30
38.47
25.65
12.82
0
CURRENT, IN MICROAMPS
38.73
48.72
58.71
68.70
78.69
88.68
SQ RT OF ELECTRODE ROTATION RATE
CD
PB

Figure 9

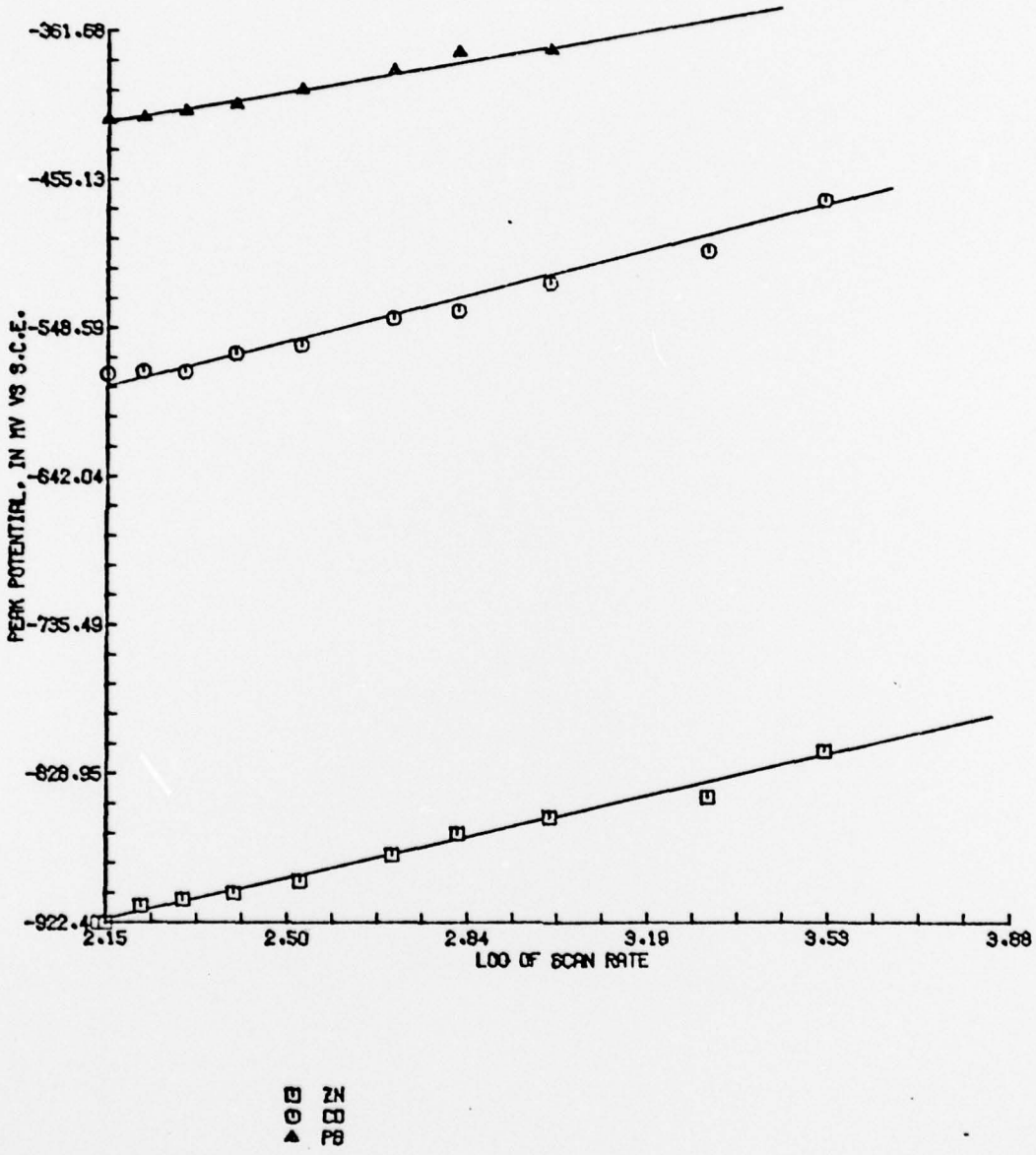
-361.68
-455.13
-548.59
-642.04
-735.49
-828.95
-922.40
PEAK POTENTIAL, IN MV VS S.C.E.
2.15
2.50
2.84
3.19
3.53
3.88
LOG OF SCAN RATE
ZN
CD
PB

Figure 10

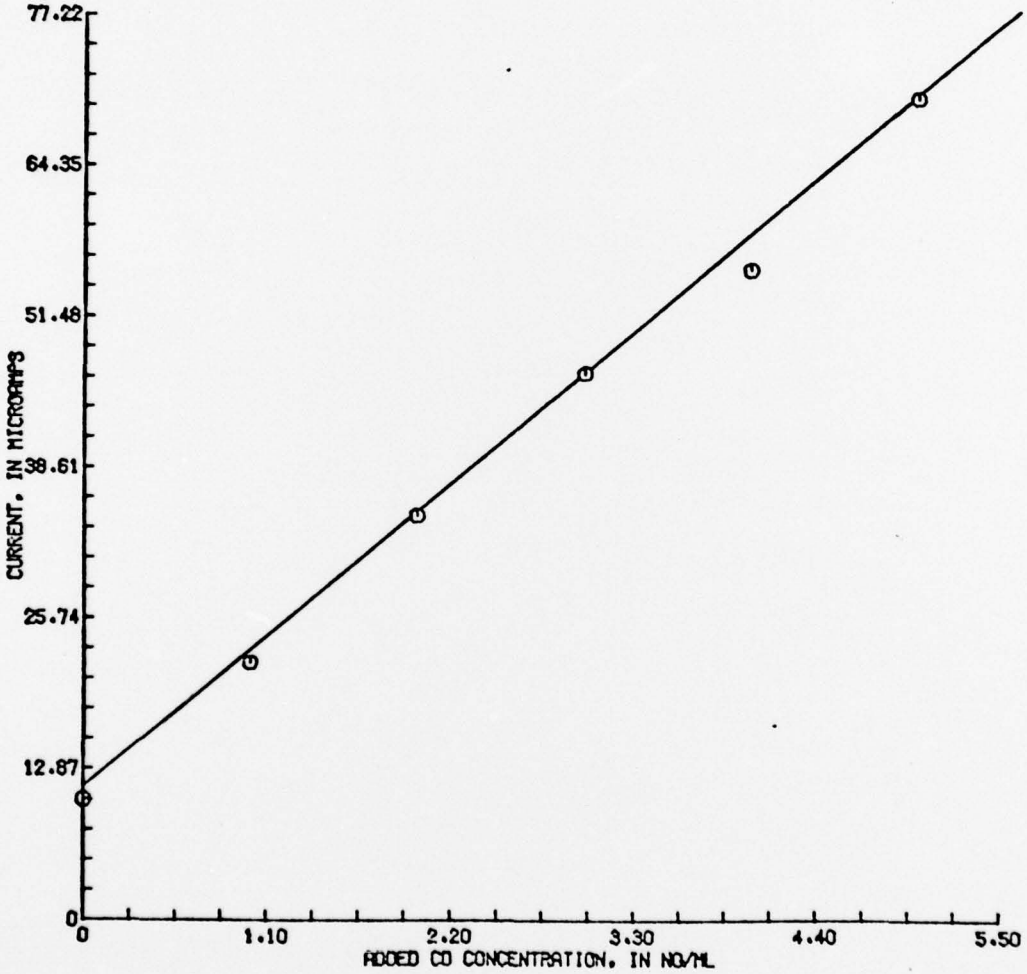
77.22
64.35
51.48
38.61
25.74
12.87
0
CURRENT, IN MICROAMPS
0
1.10
2.20
3.30
4.40
5.50
ADDED CO CONCENTRATION, IN NG/ML

Figure 11

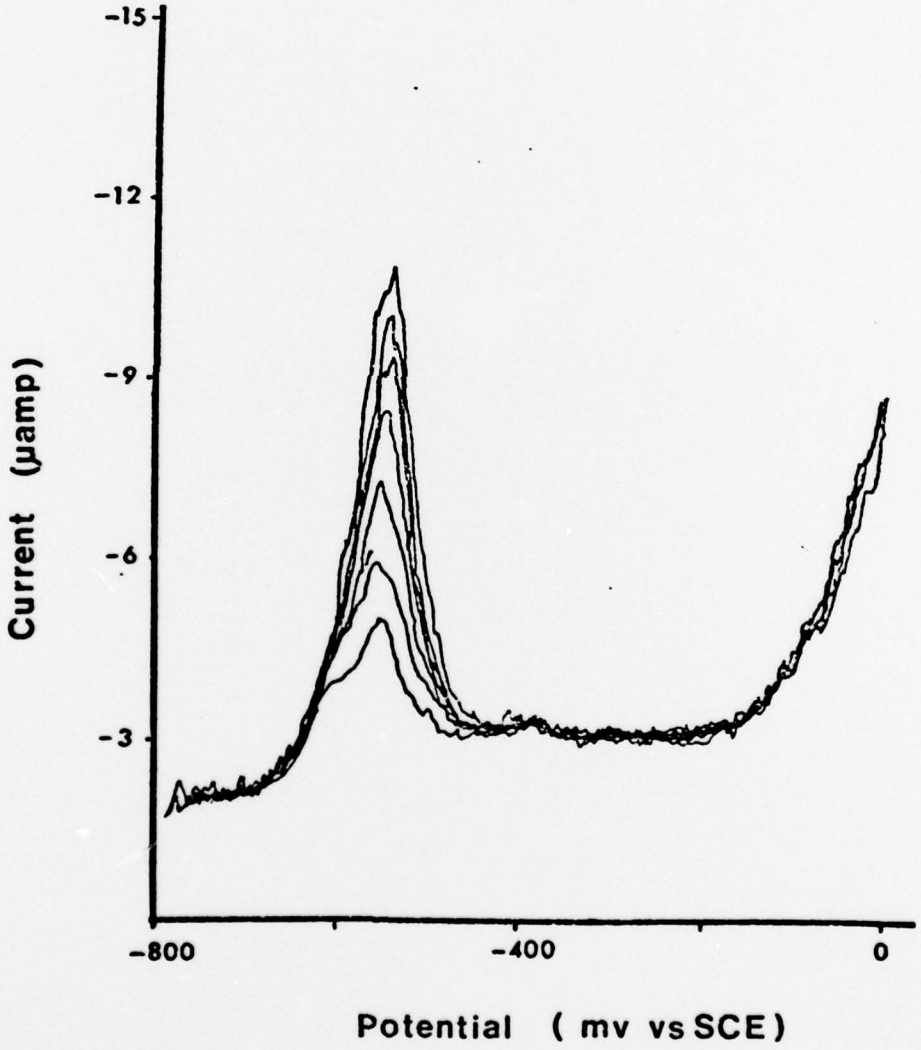

Figure 12

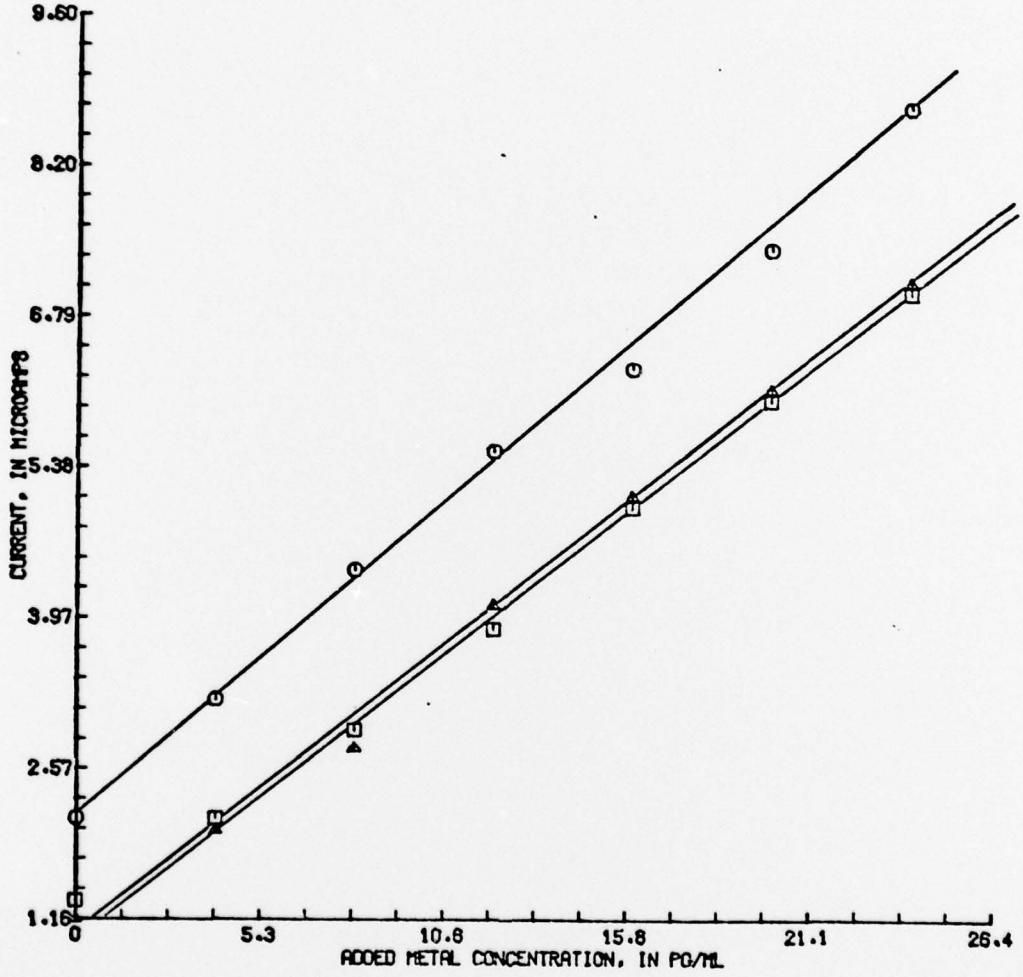
9.60
8.20
6.79
5.38
3.97
2.57
1.16
CURRENT, IN MICROAMPS
0
5.3
10.6
15.8
21.1
26.4
ADDED METAL CONCENTRATION, IN PG/ML
FOURIER TRANSFORMED PB
CD
PB

Figure 13

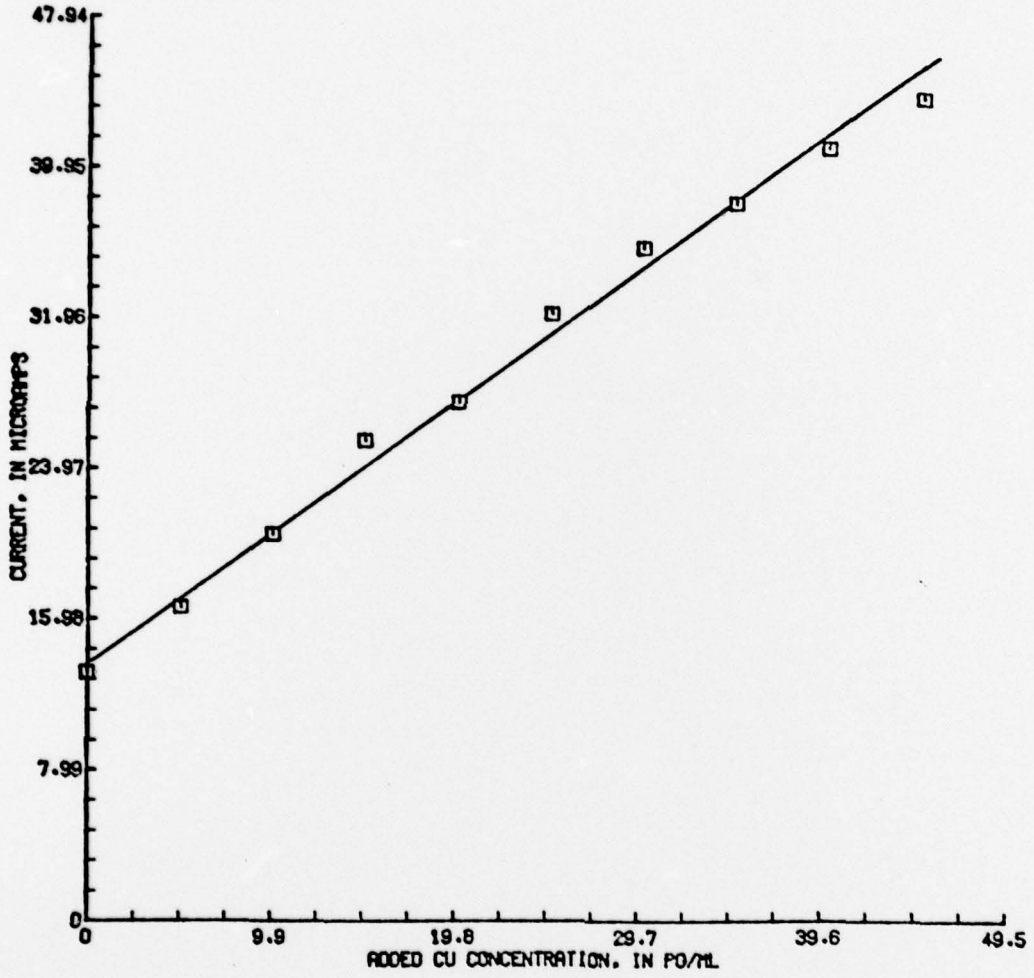
47.94
39.95
31.96
23.97
15.98
7.99
0
CURRENT, IN MICROAMPS
0
9.9
19.8
29.7
39.6
49.5
ADDED CU CONCENTRATION, IN PG/ML

Figure 14

TECHNICAL REPORT DISTRIBUTION LIST

	No. Copies
Office of Naval Research Arlington, Virginia 22217 Attn: Code 472	2
Office of Naval Research Arlington, Virginia 22217 Attn: Code 102IP 1	6
ONR Branch Office 536 S. Clark Street Chicago, Illinois 60605 Attn: Dr. Jerry Smith	1
ONR Branch Office 715 Broadway New York, New York 10003 Attn: Scientific Dept.	1
ONR Branch Office 1030 East Green Street Pasadena, California 91106 Attn: Dr. R. J. Marcus	1
ONR Branch Office 760 Market Street, Rm. 447 San Francisco, California 94102 Attn: Dr. P. A. Miller	1
ONR Branch Office 495 Summer Street Boston, Massachusetts 02210 Attn: Dr. L. H. Peebles	1
Director, Naval Research Laboratory Washington, D.C. 20390 Attn: Code 6100	1
The Asst. Secretary of the Navy (R&D) Department of the Navy Room 4E736, Pentagon Washington, D.C. 20350	1
Commander, Naval Air Systems Command Department of the Navy Washington, D.C. 20360 Attn: Code 310C (H. Rosenwasser)	1

	No. Copies
Defense Documentation Center Building 5, Cameron Station Alexandria, Virginia 22314	12
U.S. Army Research Office P.O. Box 12211 Research Triangle Park, N.C. 27709 Attn: CRD-AA-IP	1
Naval Ocean Systems Center San Diego, California 92152 Attn: Mr. Joe McCartney	1
Naval Weapons Center China Lake, California 93555 Attn: Head, Chemistry Division	1
Naval Civil Engineering Laboratory Port Hueneme, California 93041 Attn: Mr. W. S. Haynes	1
Professor O. Heinz Department of Physics & Chemistry Naval Postgraduate School Monterey, California 93940	1
Dr. A. L. Slafkosky Scientific Advisor Commandant of the Marine Corps (Code RD-1) Washington, D.C. 20380	1
Office of Naval Research Arlington, Virginia 22217 Attn: Dr. Richard S. Miller	1

TECHNICAL REPORT DISTRIBUTION LIST

	No. Copies
Dr. M. B. Denton University of Arizona Department of Chemistry Tucson, Arizona 85721	1
Dr. G. S. Wilson University of Arizona Department of Chemistry Tucson, Arizona 85721	1
Dr. R. A. Osteryoung Colorado State University Department of Chemistry Fort Collins, Colorado 80521	1
~~Dr. B. R. Kowalski~~ ~~University of Washington~~ ~~Department of Chemistry~~ ~~Seattle, Washington 98105~~	1
Dr. I. B. Goldberg North American Rockwell Science Center P.O. Box 1085 1049 Camino Dos Rios Thousand Oaks, California 91360	1
Dr. S. P. Perone Purdue University Department of Chemistry Lafayette, Indiana 47907	1
Dr. E. E. Wells Naval Research Laboratory Code 6160 Washington, D.C. 20375	1
Dr. D. L. Venezky Naval Research Laboratory Code 6130 Washington, D.C. 20375	1
Dr. H. Freiser University of Arizona Department of Chemistry Tucson, Arizona 85721	

8

	No. Copies
Dr. Fred Saalfeld Naval Research Laboratory Code 6110 Washington, D.C. 20375	1
Dr. H. Chernoff Massachusetts Institute of Technology Department of Mathematics Cambridge, Massachusetts 02139	1
Dr. K. Wilson University of California, San Diego Department of Chemistry La Jolla, California 92037	1
Dr. A. Zirino Naval Undersea Center San Diego, California 92132	1
Dr. John Duffin United States Naval Post Graduate School Monterey, California 93940	1
Dr. G. M. Hieftje Department of Chemistry Indiana University Bloomington, Indiana 47401	1
Dr. Victor L. Rehn Naval Weapons Center Code 3813 China Lake, California 93555	1
Dr. Christie G. Enke Michigan State University Department of Chemistry East Lansing, Michigan 48824	1

8